Quaternary Science Reviews 190 (2018) 20–38

Contents lists available at ScienceDirect

Quaternary Science Reviews

journal homepage: www.elsevier.com/locate/quascirev

Centennial-scale vegetation dynamics and climate variability in SE Europe during Marine Isotope Stage 11 based on a pollen record from Lake Ohrid

Ilias Kousis [a], Andreas Koutsodendris [a, *], Odile Peyron [b], Niklas Leicher [c], Alexander Francke [c, d], Bernd Wagner [c], Biagio Giaccio [e], Maria Knipping [f], Jörg Pross [a]

[a] Paleoenvironmental Dynamics Group, Institute of Earth Sciences, Heidelberg University, Im Neuenheimer Feld 234, 69120 Heidelberg, Germany
[b] ISEM, Université de Montpellier, CNRS, IRD, EPHE, Montpellier, France
[c] Institute of Geology and Mineralogy, University of Cologne, Zülpicher Str. 49a, 50674 Cologne, Germany
[d] Wollongong Isotope Geochronology Laboratory, School of Earth and Environmental Sciences, University of Wollongong, Wollongong, NSW 2522, Australia
[e] Istituto di Geologia Ambientale e Geoingegneria, CNR, Via Salaria km 29.300, 00115 Monterotondo, Rome, Italy
[f] Institute of Botany, University of Hohenheim, Garbenstr. 30, 70599 Stuttgart, Germany

ARTICLE INFO

Article history:
Received 4 October 2017
Received in revised form
27 March 2018
Accepted 2 April 2018
Available online 7 May 2018

Keywords:
Marine Isotope Stage 11
Lake Ohrid
Balkan Peninsula
Southern Europe
Eastern Mediterranean region
Abrupt climate change
Pollen-based climate reconstructions
Tephrostratigraphy
Vico tephra
Terrestrial ecosystems

ABSTRACT

To better understand climate variability during Marine Isotope Stage (MIS) 11, we here present a new, centennial-scale-resolution pollen record from Lake Ohrid (Balkan Peninsula) derived from sediment cores retrieved during an International Continental Scientific Drilling Program (ICDP) campaign. Our palynological data, augmented by quantitative pollen-based climate reconstructions, provide insight into the vegetation dynamics and thus also climate variability in SE Europe during one of the best orbital analogues for the Holocene. Comparison of our palynological results with other proxy data from Lake Ohrid as well as with regional and global climate records shows that the vegetation in SE Europe responded sensitively both to long- and short-term climate change during MIS 11. The chronology of our palynological record is based on orbital tuning, and is further supported by the detection of a new tephra from the Vico volcano, central Italy, dated to 410 ± 2 ka. Our study indicates that MIS 11c (~424–398 ka) was the warmest interval of MIS 11. The younger part of the interglacial (i.e., MIS 11b–11a; ~398–367 ka) exhibits a gradual cooling trend passing over into MIS 10. It is characterized by considerable millennial-scale variability as inferred by six abrupt forest-contraction events. Interestingly, the first forest contraction occurred during full interglacial conditions of MIS 11c; this event lasted for ~1.7 kyrs (406.2–404.5 ka) and was characterized by substantial reductions in winter temperature and annual precipitation. Most notably, it occurred ~7 ka before the end of MIS 11c and ~15 ka before the first strong ice-rafted debris event in the North Atlantic. Our findings suggest that millennial-scale climate variability during MIS 11 was established in Southern Europe already during MIS 11c, which is earlier than in the North Atlantic where it is registered only from MIS 11b onwards.

1. Introduction

In light of present anthropogenic climate change, the study of past interglacials provides a promising avenue towards improved predictions of future climate change and its consequences for the biotic and abiotic environment (e.g., Past Interglacials Working Group of PAGES, 2016). Marine Isotope Stage (MIS) 11 has received special attention in these efforts because it represents one of the best orbital analogues for present climate based on the low eccentricity and muted influence of precession (Loutre and Berger, 2003; Müller and Pross, 2007; Ruddiman, 2005; Yin and Berger, 2015). Ice-core data from Antarctica (e.g., Jouzel et al., 2007; Pol et al., 2011) as well as marine (e.g., Barker et al., 2015; Martrat et al., 2007; McManus et al., 2003; Oppo et al., 1998; Voelker et al., 2010) and terrestrial proxy records (e.g., de Vernal and Hillaire-Marcel, 2008; Melles et al., 2012; Prokopenko et al., 2002) suggest that MIS 11 was characterized by exceptionally

* Corresponding author.
E-mail address: andreas.koutsodendris@geow.uni-heidelberg.de (A. Koutsodendris).

https://doi.org/10.1016/j.quascirev.2018.04.014
0277-3791/

long-lasting (~30 kyrs) warm conditions that spanned two insolation peaks. Compared to other Quaternary interglacials, MIS 11 is the only one during which high CO_2 (270–285 p.p.m.v.; Lüthi et al., 2008) and CH_4 (600–700 p. p.b.v.; Loulergue et al., 2008) concentrations prevailed for more than 20 kyrs.

Terrestrial climate-proxy data for MIS 11 suggest a prevalence of exceptionally warm and wet conditions in the high latitudes of the Northern Hemisphere; for instance, pollen data document the presence of boreal forests in the Siberian Arctic (Melles et al., 2012) and on southern Greenland (de Vernal and Hillaire-Marcel, 2008). The higher number of terrestrial climate-proxy records available for the mid-latitudes allows identification of a considerable spatial complexity. Whereas warm and wet conditions prevailed across Europe (see reviews by Candy et al., 2014, and de Beaulieu et al., 2001), extreme droughts occurred in the southern part of North America (e.g., Valles Caldera, New Mexico – Fawcett et al., 2011). Pronounced climate instability during MIS 11 on both centennial (Koutsodendris et al., 2010; Prokopenko et al., 2010; Tye et al., 2016) and millennial (Oliveira et al., 2016; Tzedakis et al., 2009) timescales has been documented in several terrestrial records from Eurasia, further suggesting that MIS 11 climate was also temporally highly complex (Kleinen et al., 2014). The origin of these climate instabilities has been related to the weakening of the Atlantic Meridional Overturning Circulation (AMOC; e.g., Barker et al., 2015; McManus et al., 2003; Oppo et al., 1998) and associated ocean-atmosphere interactions (e.g., Billups et al., 2004; Oliveira et al., 2016).

The response of terrestrial ecosystems to climate forcing during MIS 11 has remained insufficiently constrained despite the emergence of new terrestrial records over the past years. In particular, the impact of short-term climate variability on terrestrial ecosystems (and, by extension, the dynamics of short-term terrestrial climate variability itself) during MIS 11 is yet poorly understood due to the low spatial coverage of continuous, high-resolution pollen records. The pollen records for MIS 11 in Central and NW Europe (e.g., Lake Ossowka – Nitychoruk et al., 2005; Dethlingen – Koutsodendris et al., 2010; Marks Tey – Tye et al., 2016) cover only parts of the interglacial owing to the obliteration of the respective archives by advancing glaciers. Moreover, plant migration lags complicate the reconstruction of short-term climate change in Western and Central Europe under boundary conditions other than during full interglacials (Koutsodendris et al., 2012; Müller et al., 2003). In contrast, pollen records from the Mediterranean region can provide high-fidelity information on short-term climate change throughout the Quaternary because glacial advances did not affect the respective archives. At the same time, they were also located within or in close proximity to glacial tree refugia (Medail and Diadema, 2009), which minimizes the time lag between climatic forcing and vegetation response as it may result from taxon-specific migration times. However, the yet available MIS 11 pollen records from southern Europe, such as from Greece (Tenaghi Philippon – Pross et al., 2015, and references therein; Wijmstra and Smit, 1976; Ioannina – Tzedakis et al., 2001; Kopais – Okuda et al., 2001; Megalopolis – Okuda et al., 2002), France (Praclaux; Reille et al., 2000), and Asia Minor (Lake Van; Litt et al., 2014) are of relatively low temporal resolution and therefore can only provide limited insight into short-term climate and ecosystem change. Crucial information on terrestrial climate and vegetation dynamics during MIS 11 has become available from the Iberian margin off Portugal, i.e., core MD01-2447 (Desprat et al., 2005), core MD01-2443 (Tzedakis et al., 2009), and IODP Site U1385 (Oliveira et al., 2016). However, the pollen records from the former two sites do not span the MIS 12/11 transition, and the temporal resolution of the pollen record from the latter site is compromised by low sedimentation rates across the MIS 12/11 transition and during the early part of MIS 11c. Therefore, these records do not cover the full range of climate variability connected to MIS 11.

Because continuous, highly resolved records that cover the onset, course and termination of MIS 11 are required in order to fully appreciate the evolution of this critical interval of the Quaternary, we have palynologically analyzed new core material covering MIS 11 from Lake Ohrid (SW Balkan Peninsula; Fig. 1). The cores were retrieved within an International Continental Scientific Drilling Program (ICDP) campaign in 2013 (Wagner et al., 2017). Previous studies have demonstrated the sensitive response of both the aquatic ecosystems of Lake Ohrid and the terrestrial ecosystems in the catchment area of the lake to climate change on sub-orbital (e.g., Lézine et al., 2010; Vogel et al., 2010; Wagner et al., 2010) and orbital timescales (Francke et al., 2016; Just et al., 2016; Sadori et al., 2016).

For the purpose of this study, we have used core material from the DEEP site that extends continuously back to at least 1.3 Ma (Wagner et al., 2017) and hence also covers MIS 11. To unravel the terrestrial ecosystem response to abrupt climate change and to reconstruct the magnitude of climate change at Lake Ohrid during MIS 11, we have increased the temporal resolution of previously published pollen information spanning this interval (Bertini et al., 2016; Sadori et al., 2016) by four times and generated quantitative pollen-based climate estimates from our data. We integrate our new centennial-scale-resolution pollen record with previously published sedimentological and oxygen-isotope data from the DEEP Site (Francke et al., 2016; Lacey et al., 2016). Finally, we compare our results with (supra)regional proxy records both from the marine and terrestrial realms in order to shed light on the character and timing of short-term climate change during MIS 11.

2. Regional setting

Located in a N-S-trending tectonic graben on the southwestern Balkan Peninsula, Lake Ohrid is surrounded by the Mokra mountains to the west (maximum altitude: 1514 m above sea level [a.s.l.]) and the Galičica mountains to the east (2265 m a.s.l.). The lake is situated at an altitude of 693 m a.s.l. and is up to 289 m deep (Wagner et al., 2017). It has a surface area of 358 km^2, a water volume of ~50.7 km^3 (Matzinger et al., 2007), and a direct catchment area of 1310 km^2 (Wagner et al., 2010).

Climatically, the Lake Ohrid region is influenced predominantly by high- and mid-latitude climate systems of the Northern Hemisphere (i.e., Westerlies, Siberian High; Fig. 1). It is characterized by typical Mediterranean climate conditions, marked by wet and cold winters (with the occurrence of frost), and dry and warm summers (Lionello et al., 2006, and references therein). During winter, moisture delivery is mainly linked to increased convective precipitation (Bosmans et al., 2015) and the penetration of westerly storm tracks across the Mediterranean region (e.g., Xoplaki et al., 2004); cold spells are related to southward outbreaks of polar air masses from the Russian/Siberian High (e.g., Saaroni et al., 1996). Meteorological data acquired during the 1961–1990 period from the meteorological stations at the towns of Ohrid and Resen (about 20 km east of Lake Ohrid) have yielded a mean annual precipitation between 698 and 1194 mm yr^{-1} (average: 907 mm yr^{-1}). The mean annual air temperature is 11.1 °C, with minimum and maximum temperatures of −5.7 and 31.5 °C, respectively (Popovska and Bonacci, 2007).

Today, Lake Ohrid is surrounded by forest vegetation that consists predominantly of Mediterranean and Balkan elements, while several central European taxa are also present (Čarni and Matevski, 2015; Matevski et al., 2011; Panagiotopoulos et al., 2013). The riparian forests around Lake Ohrid are dominated by *Salix alba*. Deciduous and semi-deciduous oaks (e.g., *Quercus cerris, Q. frainetto,*

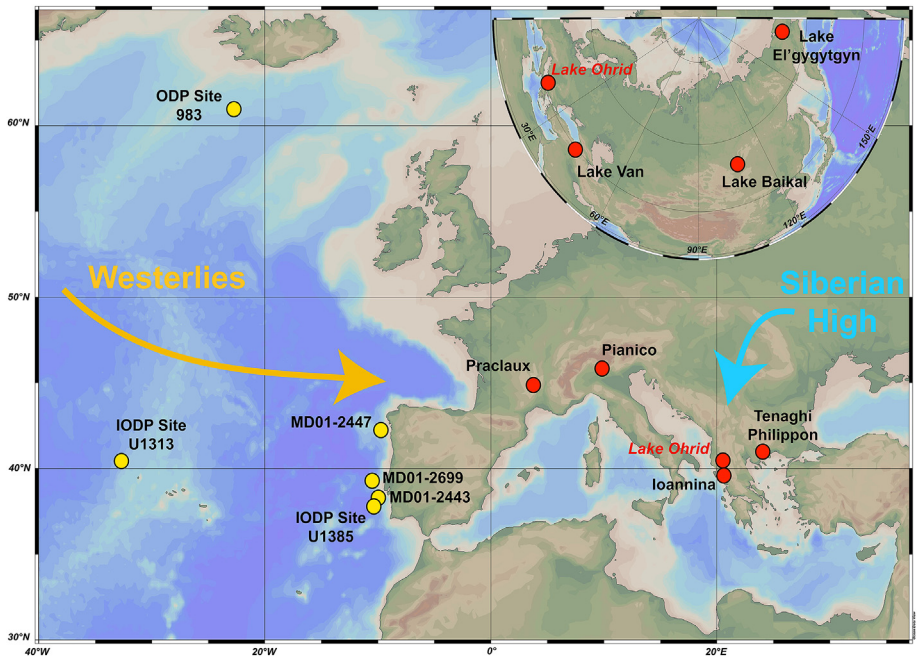

Fig. 1. Locations of Lake Ohrid in SE Europe and of selected other proxy records for MIS 11 from the greater Mediterranean region, the North Atlantic and Siberia as discussed in the text. The major climatic systems influencing the area of Lake Ohrid on orbital timescales are also shown.

Q. petraea, Q. pubescens, and *Q. trojana*) and hornbeams (*Carpinus orientalis, Ostrya carpinifolia*) dominate the forests up to 1600 m. Mesophilous (*Acer obtusatum, Carpinus betulus, Corylus colurna*) and montane species (e.g., *Abies borisii-regis* and *Fagus sylvatica*) dominate up to 1800 m, and alpine pasturelands and grasslands thrive above the timberline (~1900 m). The western part of the lake is surrounded by steep slopes, which in the past have been grazed and are now gradually being reforested. Sparse populations of *Pinus peuce* and *P. nigra*, considered to represent Tertiary relics (Čarni and Matevski, 2015; Sadori et al., 2016), exist in the region of Lake Ohrid. Finally, Lake Ohrid itself has a rich macrophytic flora dominated by *Phragmites australis*, *Lemna triscula*, *Myriophyllum* spp., *Potamogeton* spp., and *Chara* spp. (Imeri et al., 2010).

3. Material and methods

3.1. Sampling and palynological analysis

Palynological samples were taken from cores recovered at the DEEP Site (ICDP Site 5045–1; 41°02′57″ N, 20°42′54″ E), which was drilled in the center of the lake at a water depth of 243 m. In total, 118 palynological samples were analyzed at 16 cm resolution for the interval 157.87–176.11 m composite depth (mcd), and at 64 cm resolution for the interval 155.95–157.87 mcd. Based on the age model (see Section 4.1) for the DEEP Site, this sampling corresponds to an average temporal resolution of 477 yrs (range: 406–650 yrs) and 2390 yrs for the 155.95–157.87 mcd and 155.95–157.87 mcd intervals, respectively. The 32 low-resolution samples that had previously been published by Sadori et al. (2016) were reprocessed and recounted.

From each sample, a sediment volume of 1.3 cm^3 was subjected to palynological processing. The processing included spiking with two tablets of *Lycopodium* marker spores (Lund University, batch numbers 1031 [20848 ± 1546 spores/tablet] and 483216 [18583 ± 1708 spores/tablet]), treatment with HCL (10%) and HF (40%), sieving through a 7 μm mesh, and slide preparation using glycerin jelly. Slides were analyzed with a Zeiss Axioscope A1 light microscope at 400x and 630x magnification. With the exception of two samples that yielded low pollen concentrations, at least 300 pollen grains (excluding spores, pollen from aquatic plants and algae) were counted per sample (range: 245–461; mean: 320). *Pinus* pollen grains were also excluded from the counting sums because of their natural overrepresentation in Lake Ohrid (Bertini et al., 2016; Sadori et al., 2016). *Pinus* pollen grains and algae were counted until 25 *Lycopodium* marker spores were registered and subsequently extrapolated.

Pollen assemblage zones (PAZ) were defined using the CONISS application (Grimm, 1987) within the Tilia software; the definition of the pollen assemblage superzones (PASZ) follows the scheme of Sadori et al. (2016) for Lake Ohrid. Abrupt vegetation events (i.e., abrupt expansions and contractions of forest populations) were calculated as the first derivative of the arboreal pollen (AP) percentages against age. The resulting rate of change (ROC) is a useful indicator for determining abrupt changes (e.g., Fletcher et al., 2013; Milner et al., 2016), with negative and positive values marking forest contraction and expansion episodes, respectively. Considering that major climatic-induced forest setbacks in Lake Ohrid cores during the Last Interglacial exhibit a decline of ~40% in tree-pollen percentages (Sinopoli et al., 2018), a ROC of at least 40% within at least two consecutive samples was used in the definition of high-amplitude abrupt vegetation events during MIS 11 in our study.

3.2. Quantitative paleoclimate reconstructions

To obtain quantitative information on paleoclimatic change during MIS 11 at Lake Ohrid, we applied the modern analogue technique (MAT; Guiot, 1990; Overpeck et al., 1985) to our pollen dataset. This technique has been previously applied to pollen records from the Eastern Mediterranean region in order to reconstruct abrupt climate change during the last glacial-interglacial cycle (Kotthoff et al., 2011; Peyron et al., 2011; 2017; Pross et al., 2009). It has also been applied to several MIS 11 pollen records from the Iberian margin (Desprat et al., 2005), the western French

Alps (Field et al., 2000), Lake Biwa (Japan; Tarasov et al., 2011), and Lake El'gygytgyn (Arctic Siberia; Melles et al., 2012). The MAT is based on the comparison of fossil and modern pollen assemblages using a dissimilarity index. For each fossil pollen assemblage, five modern pollen assemblages from a database containing modern pollen spectra from a wide range of climatic zones are selected as the closest analogues; based on the climate data known for these analogues, estimates with regard to various climate parameters can be obtained for each fossil assemblage. The MAT reconstructions as carried out here rely on a database that comprises more than 3000 surface pollen samples from a wide variety of biomes across Eurasia and NW Africa (Peyron et al., 2017). The climate parameters reconstructed in this study are the mean temperature of the coldest month (MTCO), number of growing-degree days per year (i.e., the annual sum of growing temperatures for days above 5 °C (GDD5), mean annual temperature (TANN), and mean annual precipitation (PANN).

3.3. Preparation and geochemical analysis of tephra samples

For the separation of tephra shards from their host sediment about 0.5 g of freeze-dried sediment were treated with 10% HCl for 12 h to remove carbonates, and subsequently sieved with 80 and 25 μm nylon meshes (Blockley et al., 2005). The 80–25 μm fraction was split into three density fractions (<2.3 g/cm^3, 2.3–2.5 g/cm^3, and >2.5 g/cm^3) using sodium polytungstate (SPT) as a heavy liquid. The 2.3–2.5 g/cm^3 and >2.5 g/cm^3 fractions were mounted separately on microscope slides for inspection using a ZEISS Axiolab A1 petrographic microscope. The concentration of glass shards was calculated by normalizing the counted glass-shard values for 1 g of dried sediment.

For geochemical analysis, glass shards were mounted on an epoxy puck, polished, and carbon coated for wavelength dispersive spectrometry (WDS) microprobe analysis. Individual glass shards and reference standards were measured at the University of Cologne using a JEOL JXA-8900RL Electron Microprobe equipped with a five-wavelength dispersive spectrometer, which was set to 12 keV accelerating voltage, 6 nA beam current, and 5 μm beam diameter, respectively. Detailed settings such as counting times, measuring order, and reference materials used for calibration are given in the supplementary material along with the full analytical details of the individual measurements. All geochemical compositions were recalculated as being 100% water free, excluding volatiles (Cl, SO_3, and F).

4. Chronology

4.1. Development of age model

The age model of the DEEP cores for the past 637 ka is based on tephrochronology (Leicher et al., 2016), with eleven tephra layers being used as first-order tie points, and the tuning of biogeochemical proxy data (i.e., total organic carbon [TOC] and total nitrogen [TN]) to orbital parameters as second-order tie points (Francke et al., 2016)(see also Supplementary Information). In the following, we briefly describe the individual steps in the development of the Francke et al. (2016) age model; for an in-depth discussion the reader is referred to the original paper. The tephrostratigraphic tie points were used to define the cross-correlation points with orbital parameters, with the ages of tephra layers Y-5 (39.6 ± 0.1 ka), X-6 (109 ± 2 ka), P-11 (133.5 ± 2 ka), and A11/12 (511 ± 6 ka) corresponding to inflection points of increasing summer insolation (21st June) and increasing winter-season length (September to March equinoxes) at the latitude of Lake Ohrid (i.e., 41°N). The stratigraphic positions of the aforementioned tephra layers coincide with pronounced minima in the TOC content and the TOC/TN ratio. The TOC content represents the amount of finely dispersed organic matter in the sediments of Lake Ohrid, which is mainly of aquatic origin (Lacey et al., 2015). The TOC/TN ratio is then rather used as a measure for the intensity of organic matter decomposition and mixing conditions in the water column than an indicator for the amount of allochthonous and autochthonous organic matter (Francke et al., 2016). High (low) TOC contents and TOC/TN ratios indicate a relatively high (low) nutrient supply from the catchment and relatively high (low) spring and summer temperatures; these conditions promote (reduce) the primary productivity in the water column, and moderate the decomposition of organic matter after deposition as a result of moderate (strong) mixing and long (low) winter seasons. During the time of summer insolation inflection (perihelion passage in March), summer insolation is moderate while winter season length remains extended. On this basis, the correspondence of low TOC contents and TOC/TN ratios at the time of summer insolation inflection is explained by (i) overall low summer temperatures that hamper the primary productivity in the epilimnion, and (ii) persistently long winter season that promotes mixing and decomposition of organic matter in the water column and the surface sediments (Francke et al., 2016). During perihelion passage in March the Northern Hemisphere sea-ice extent is near its maximum (Berger et al., 1981) and leads to overall cold and dry conditions in the Mediterranean region (e.g., Tzedakis et al., 2003, 2006).

According to this age model, the MIS 11 interval spans from 174.19 mcd (~424 ka) to 157.87 mcd (~367 ka) in the DEEP composite record. The robustness of the age model for the MIS 11 interval of the DEEP cores as outlined above is confirmed by new, strictly independent tephrostratigraphic results (compare Section 4.2). To facilitate comparison with previously published records spanning MIS 11, we here follow the scheme of Tzedakis et al. (2001) for terrestrial records in Europe; accordingly, we have divided the interglacial into three substages, i.e., MIS 11c (~424–398 ka), 11b (~398–390 ka) and 11a (~390–367 ka).

4.2. MIS 11c tephra layer

To critically assess the reliability of the age model for the MIS 11 interval as discussed above, we have carried out tephrostratigraphic analyses on the MIS 11 part of the DEEP cores, thereby following up on the identification of volcanic glass shards at 170.04 mcd depth during lower-resolution grain-size analyses. To identify the exact stratigraphic position of the tephra layer, the sediments between 171.14 and 169.92 mcd were sub-sampled in 2-cm-thick intervals for cryptotephra analysis. The resulting glass-shard concentration across this part of the core shows a clear unimodal distribution with a peak at 170.06–170.04 mcd (see Supplementary Information). The bottom depth of this interval (i.e., 170.06 mcd) was set as the isochron position marking the time of deposition. The presence of glass shards below 170.06 mcd is most likely related to the *in-situ* downward mobilization of shards by bioturbation and/or sedimentary gravitational processes (e.g., Payne and Gehrels, 2010; Wulf et al., 2018); the occurrence of glass shards above 170.04 mcd can likely be linked to erosional processes in the catchment area of the lake and subsequent transport to the DEEP site.

The newly detected tephra, labeled OH-DP-1700.6 following the nomenclature of the Lake Ohrid DEEP core tephra layers (Leicher et al., 2016), has a distinct K-rhyolitic composition (Fig. 2). Stratigraphically, it is located within MIS 11c as inferred by available sedimentological and geochemical data from the DEEP cores (Wagner et al., 2017) and our palynological data (see Section 5.1;

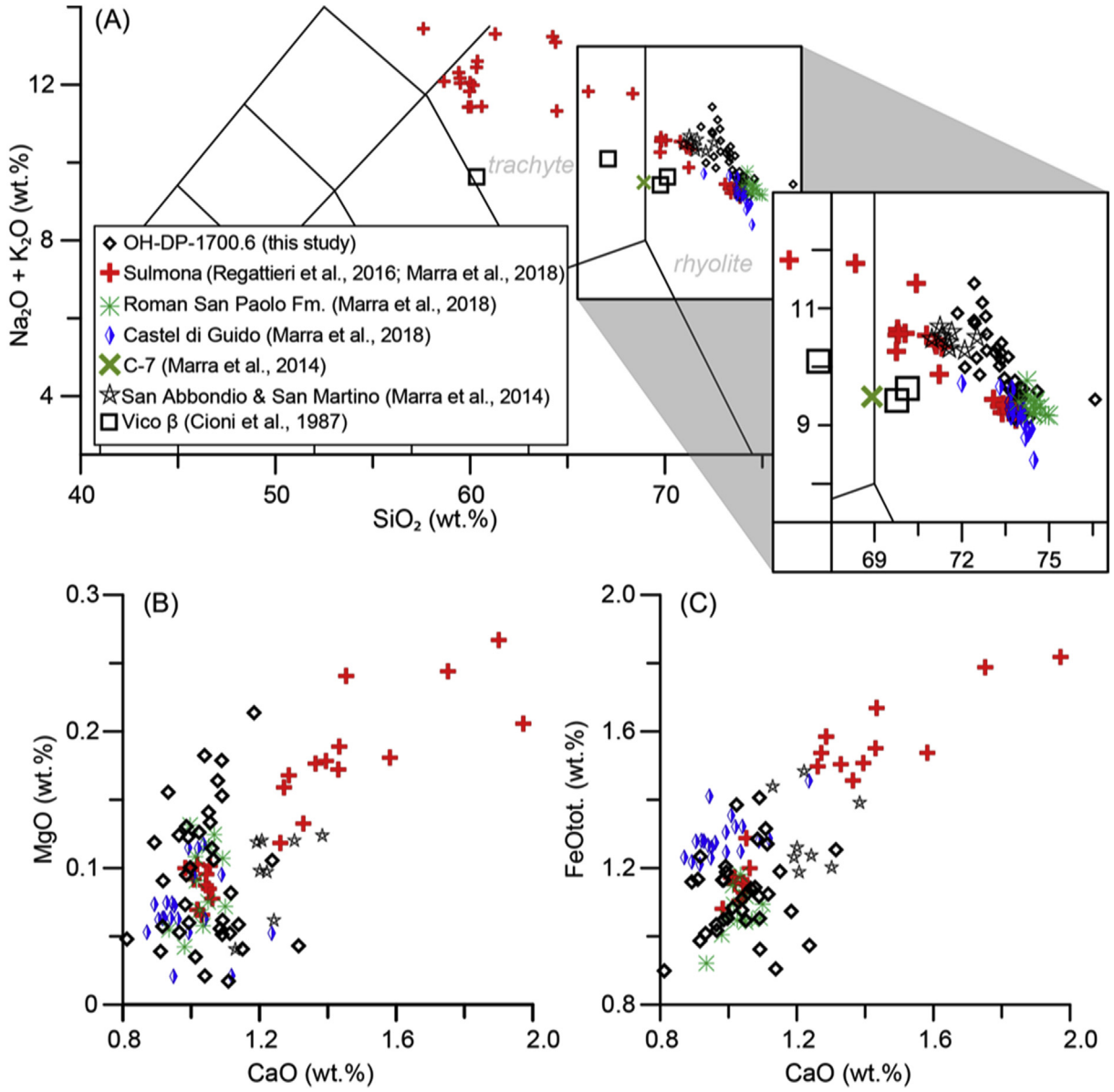

Fig. 2. Comparison of the geochemical glass composition of the Lake Ohrid tephra OH-DP-1700.6 with proximal and distal deposits of the trachytic-rhyolitic tephra from the Vico β eruption. A) TAS diagram after Le Bas et al. (1986), classifying the studied tephra layers. The data for sample C-7 (Marra et al., 2014) are based on Fusion ICP-MS bulk analysis; the data of Vico β (Cioni et al., 1987) are based on XRF analysis; all other samples were measured by EMPA-WDS. B) and C) Bi-oxide plots for the tephra OH-DP-1700.6 and the evolved parts of the Vico equivalents (see also additional plots in Supplementary Information).

Fig. 3). It is also located upcore with respect to the OH-DP-1817 tephra, which is derived from the Pozzolane Rosse eruption at c. 457 ka, i.e., during MIS 12 (Leicher et al., 2016).

The K-rhyolitic composition and the eruption date during MIS 11 points to an early activity phase of the Vico volcano in Italy. The only examples of rhyolitic tephra of the peri-Tyrrhenian ultra-potassic volcanism during MIS 11 comprise Vico β (Cioni et al., 1987), Tufi Stratificati Varicolori Vicani (Barberi et al., 1994), and Rio Ferriera Formation, Vico Period I (Perini et al., 2004). A correlation to the rhyolitic-trachytic tephra from the Vico volcano is confirmed by comparison of the new OH-DP-1700.6 geochemical data from Lake Ohrid with available data from proximal and distal sites (Fig. 2). The proximal sites include (i) the trachytic-rhyolitic Plinian fallout deposits of the Vico β eruption (Cioni et al., 1987), matching the rhyolitic bedded pumice layers from the San Abbondio and San Martino sections east of the Vico volcano (Marra et al., 2014; erroneously labeled as Vico α, Fabrizio Marra, pers. comm. 2018); (ii) the high-silica trachytic, near-rhyolitic "Bedded Pumice" deposits of the San Paolo Formation around the city of Rome occurring in the aggradational succession of MIS 11 high-stand sea-level (sample C-7; Marra et al., 2014, 2016) and; (iii) the rhyolitic to trachytic deposits from the Castel di Guido and Roman San Paolo Formations (Marra et al., 2018). The distal sites comprise the MIS 11c lacustrine successions of the Sulmona Basin (Regattieri et al., 2016) and palustrine sediments of the Arno Valley, Tuscany (Bigazzi et al., 1994).

The best currently available radioisotopic age for this widespread Vico tephra is provided by the $^{40}Ar/^{39}Ar$ dating of the C-7 sample from the San Paolo Formation, which yielded an age of 410 ± 2 ka (Karner et al., 2001). New, yet unpublished $^{40}Ar/^{39}Ar$ dates for the Vico trachytic-rhyolitic tephra layer from the Sulmona Basin and the Roman area further confirm this age (Sébastien

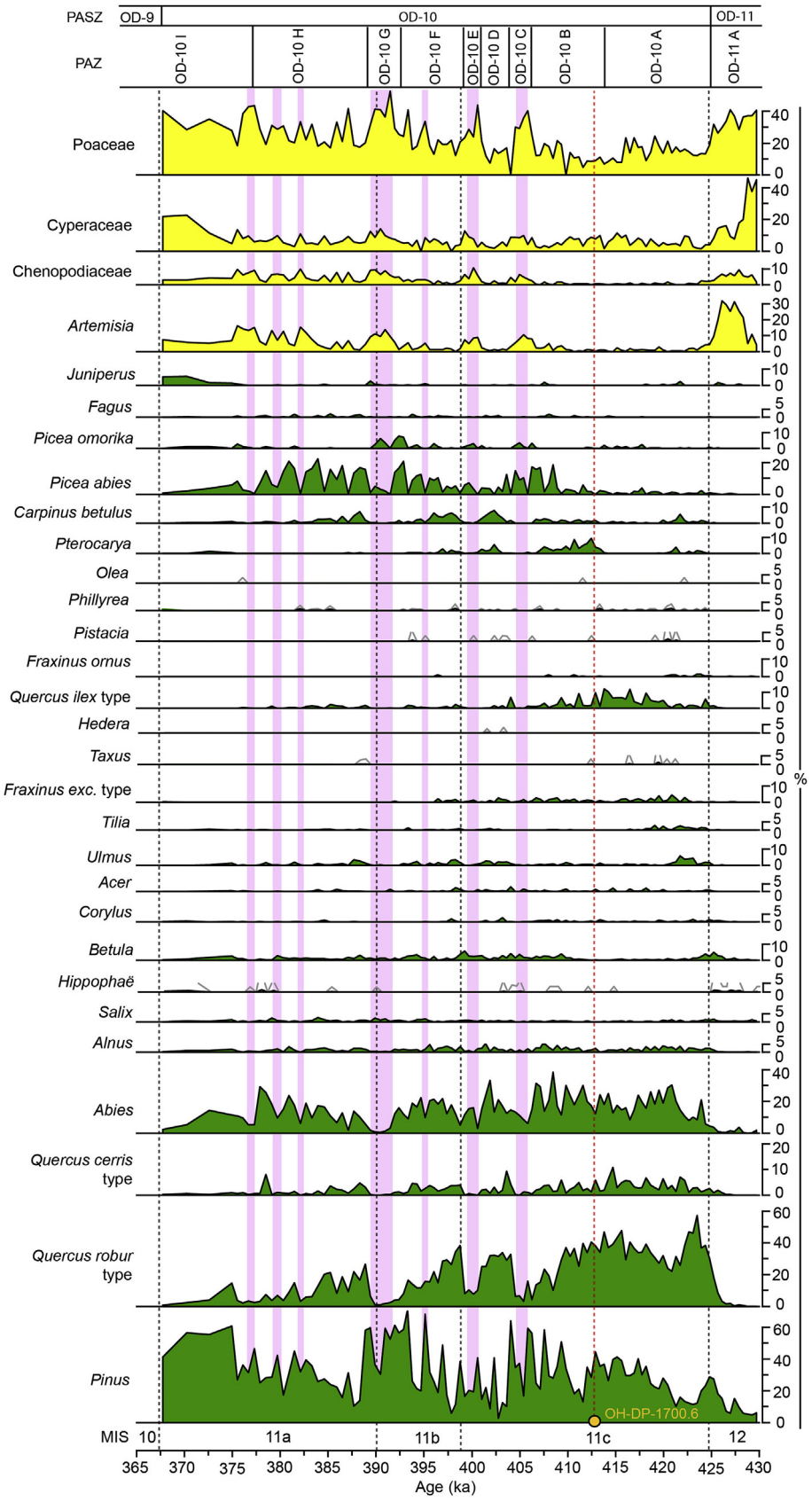

Fig. 3. Selected pollen taxa (arboreal taxa in green, non-arboreal taxa in yellow) from MIS 11 at Lake Ohrid plotted against age. Pink bands represent the most prominent forest contraction events (compare Fig. 4). Black dashed lines represent MIS boundaries. The OH-DP-1700.6 tephra at 170.06 mcd is indicated with a red dashed line. Note 10x exaggeration lines for *Hedera*, *Hippophaë*, *Olea*, *Phillyrea*, *Pistacia* and *Taxus*. PAZ: Pollen assemblage zones; PASZ: Pollen assemblage superzones. (For interpretation of the references to color in this figure legend, the reader is referred to the Web version of this article.)

Nomade, pers. comm. 2018). A younger age (i.e., 403 ± 6 ka) has been reported for a sample from Tufi Stratificati Varicolori Vicani (i.e., TSVVβ) also based on $^{40}Ar/^{39}Ar$ dating (Barberi et al., 1994), presumably matching the Vico β eruption (Cioni et al., 1987) and, thus OH-DP-1700.6. However, we refrain to adopt this age because of the lack of analytical details with regard to the $^{40}Ar/^{39}Ar$ dating of the TSVVβ sample, which preclude recalculations with a currently accepted flux standard and ^{40}K decay constant. Instead, the age of 410 ± 2 ka (Karner et al., 2001) was determined using the same flux standard and ^{40}K decay constant as for the calculations of the tephra ages in the DEEP core (Francke et al., 2016; Leicher et al., 2016), which allows for optimum comparability of the results.

An age of 410 ± 2 ka for the OH-DP-1700.6 tephra fully supports the age model of Francke et al. (2016) for the Lake Ohrid DEEP core as presented above. According to that chronology, the position of the OH-DP-1700.6 tephra at 170.06 mcd would be equivalent to an age of 412.9 ± 2 ka. Thus, the finding of volcanic glass shards from the Vico rhyolite eruption does not only yield an independent validation of the previously established age model for the DEEP record, but also provides critical age control with regard to the timing of the vegetation changes registered in the Lake Ohrid cores during MIS 11.

5. Results

5.1. Palynostratigraphical characteristics of MIS 11 at Lake Ohrid

The palynological record for MIS 11 from the DEEP site comprises ten pollen zones, i.e., PAZs OD-11 A to OD-10 A-I (Fig. 3). The transition between MIS 12 and 11 (OD-11 A) marks the expansion of forests at the expense of steppe and grassland communities as portrayed by the increase of AP percentages from 6 to 80% and the coeval decrease of *Artemisia*, Chenopodiaceae, Cyperaceae, and Poaceae (Figs. 3 and 4). The MIS 11c substage (equivalent to PAZs OD-10 A to OD-10 E) is marked by the establishment of forests in the catchment area of Lake Ohrid. The period between 424.4 and 414.3 ka (PAZ OD-10 A) is dominated by deciduous temperate forests that included mesophilous (i.e., *Acer, Carpinus betulus, Carya, Corylus, Ostrya, Pterocarya, Quercus robur* and *Q. cerris* types, *Tilia*, and *Ulmus*) and Mediterranean taxa (i.e., *Fraxinus ornus*, *Olea*, *Phillyrea*, *Pistacia*, and *Quercus ilex* type). The period between 414.3 and 406.2 ka (PAZ OD-10 B) exhibits the highest AP percentages within the entire record, peaking at 89% at 409.8 ka. Although this period is again dominated by temperate forests, it also exhibits increasing abundances of conifers including *Abies*, *Picea abies*, and *Pinus* (Fig. 3). The short interval between 406.2 and 404.5 ka (PAZ OD-10 C) is marked by a strong forest demise as inferred by a drop of AP from 77 to 31% and an increase of steppic elements and grasses (Figs. 3 and 4). This interval represents the first forest contraction during MIS 11 as documented in the Lake Ohrid record (here termed LO-11-1); it lasted for ~1.7 kyrs (Table 1; Fig. 4).

The interval from 404.5 to 401.0 ka (PAZ OD-10 D) documents the recovery of temperate forests after the LO-11-1 event; these forests were dominated by *Quercus robur* type, *Abies* and *Carpinus betulus* (Fig. 3). The interval from 401.0 to 399.2 ka (PAZ OD-10 E) is characterized by the strongest forest contraction in the entire record (i.e., LO-11-2); the contraction event is expressed by an AP drop from 87 to 22% (Table 1; Figs. 3 and 4). At the same time, this zone marks the end of the MIS 11c substage.

Substages MIS 11b (PAZs OD-10 F [399.2–392.4 ka] and OD-11 G [392.4–389.4 ka]) and 11a (PAZs OD-10 H [389.4–377.3 ka] and OD-11 I [377.3–367.8 ka]) are characterized by a gradual decrease in AP percentages and the expansion of steppic elements and grasses (Figs. 3 and 4). The maximum percentages of mesophilous taxa (e.g., *Quercus robur* type and *Carpinus betulus*) are lower (max. 66% in PAZ OD-10 F) than during MIS 11c; at the same time, Mediterranean taxa become rare forest elements (Fig. 4). In addition, montane tree taxa reach higher percentages than mesophilous trees from the middle of PAZ OD-10 F to PAZ OD-1O I. While the percentages of *Abies* are slightly lower than during MIS 11c, those of *Picea omorika* reach up to ~8% in PAZ OD-10 G; *P. abies* attains ~22% in PAZ OD-10 H (Figs. 3 and 4). *Pinus* percentages increase throughout MIS 11b and 11a. Towards the transition to MIS 10 (PAZ OD-10 I), *Pinus* becomes the dominant forest element; *Juniperus* percentages also increase during that time (Fig. 3).

Superimposed on the gradual changes in forest composition, a series of short-term forest-contraction events (here termed LO-11-3 to LO-11-7) occurs during MIS 11b and 11a (Fig. 4). While all events are characterized by reductions in AP percentages between 11 and 38%, *Pinus* percentages remain largely unaffected and strongly drop only during LO-11-4 (Table 1; Fig. 3). In contrast, the percentages of steppic elements, grasses and sedges increase during all events, often associated with slight increases in the percentages of pioneer taxa (Fig. 4). Based on our chronology, the events are centered at 395.5, 390.2, 382.7, 379.7, and 376.7 ka, and have durations between 0.9 and 2.5 kyrs (Table 1).

5.2. Pollen-based quantitative climate reconstructions

The transition between MIS 12 and 11 is marked by abrupt increases in MTCO (−17 to −3 °C), TANN (0–7 °C) and PANN (450–600 mm). MIS 11c (424–398 ka) exhibits average values of 7.0 °C for TANN, −1.5 °C for MTCO, and 1550 °C days for GDD5 (Fig. 5). Maximum TANN and MTCO values were reached at 413 ka (12.2 and 4.4 °C, respectively; Fig. 5). Minimum TANN and MTCO values are registered during 406.2–404.5 ka (3.7 and −8.9 °C, respectively) and 401.0–399.2 ka (2.7 and −7.2 °C, respectively); they coincide with the forest contraction events LO-11-1 (PAZ OD-10 C) and LO-11-2 (PAZ OD-10 E), respectively (Table 1, Fig. 5). With regard to precipitation, PANN values are close to 800 mm on average during MIS 11c; maximum values (~950 mm) were reached at 421–418 ka and 412–407 ka, whereas minimum values occurred during the forest contraction events (~550 and 620 mm for LO-11-1 and LO-11-2, respectively; Table 1; Fig. 5).

For the interval of MIS 11b and 11a (398–367 ka), the temperature reconstructions yield lower values than for MIS 11c and show only a low-amplitude variability. In contrast, precipitation is higher and highly variable (Fig. 5). Among the forest-contraction events registered during MIS 11b and 11a, the events LO-11-4 (391.9–389.4 ka) and LO-11-5 (383.3–382.1 ka) stand out as the coldest and driest. They are characterized by minimum TANN values of 2 °C, and minimum MTCO values of −8 and −10 °C, respectively; minimum PANN values are below 600 mm (Table 1). In contrast, the forest-contraction events LO-11-3 (396–395.1 ka), LO-11-6 (380.3–379.1 ka), and LO-11-7 (377.9–375.5 ka) were characterized by slightly higher TANN (3–4 °C), MTCO (−3 to −5 °C), and PANN (>670 mm) minimum values (Table 1).

5.3. Rare vegetation elements

The presence of pollen from several rare vegetation elements in the Lake Ohrid record during MIS 11 merits special attention (Fig. 6). These rare elements include taxa that are (i) today extinct from the Lake Ohrid area (i.e., *Carya*, *Cedrus*, *Parrotia*, *Pterocarya*, *Tsuga*, and *Zelkova*; Magri et al., 2017, and references therein); (ii) present today in the area, but were rare during the Middle Pleistocene (*Castanea, Fagus, Juglans*, and *Vitis*; e.g., Griffiths et al., 2004); and (iii) Tertiary relics that still thrive on the Balkan Peninsula today (*Picea omorika*; Nasri et al., 2007).

Pterocarya (reaching as much as 10% at ~411 ka) and *P. omorika*

(7.5% at ~393 ka) are the two most common rare elements during MIS 11 at Lake Ohrid. *Fagus* (max. 2%), and *Carya* (max. <1%) are present sporadically throughout the entire MIS 11 record. Pollen from *Juglans* (<1%), *Zelkova* (<1%), *Parrotia* (<1%), *Tsuga* (<0.5%), and *Vitis* (<1%) has been found in a few samples within the MIS 11 record. Finally, single findings of *Castanea* (<1%) and *Cedrus* (<1%) pollen were registered at 375 and 399 ka, respectively.

6. Discussion

6.1. Vegetation dynamics at Lake Ohrid during MIS 11

The vegetation succession at Lake Ohrid during MIS 11c (424–398 ka) comprises three distinct intervals that reflect the typical interglacial pattern of protocratic, mesocratic and oligocratic forest phases (Andersen, 1994; Birks and Birks, 2004). Interglacial forest successions in Europe are not only controlled by the temperature increase from the onset of the interglacial onwards and the gradual temperature decrease towards the next glacial, but also depend critically on the nutrient availability in soils (Andersen, 1994; Birks and Birks, 2004; Tzedakis, 2007). Interglacial successions start typically with the expansion of pioneer trees (such as *Betula, Juniperus* and *Pinus*) that are light-demanding and can grow on nutrient-poor soils (Andersen, 1994; Birks and Birks, 2004; Tzedakis, 2007). At Lake Ohrid, this protocratic phase (~427–424 ka) is represented by the expansion of *Pinus* and *Betula,* the presence of *Hippophaë* and *Salix*, and the appearance of *Juniperus* during the MIS 12/11 transition (Fig. 3). During the subsequent mesocratic phase, forests are marked by the expansion of trees that require high temperatures and nutrient-rich soils to grow (Andersen, 1994; Birks and Birks, 2004; Tzedakis, 2007). At Lake Ohrid, this is documented between ~424 and 413 ka by the expansion of temperate (*Abies*, *Acer*, *Alnus, Corylus*, *Fraxinus excelsior* type, *Quercus robur* type, *Quercus cerris* type, *Tilia*, and *Ulmus*) and Mediterranean (*Fraxinus ornus*, *Phillyrea*, and *Quercus ilex* type) tree taxa (Fig. 3). The subsequent oligocratic phase (Andersen, 1994; Birks and Birks, 2004), which is marked by decreasing phosphorus availability in soils (Wardle et al., 2004), is reflected in the younger intervals of MIS 11c (~413–398 ka) by increases of *Pterocarya* at ~413 ka, *Picea abies* at ~408 ka, and *Carpinus betulus* at ~404 ka (Fig. 3).

Despite the recurrent pattern of vegetation successions during interglacials, the suite of tree taxa involved in these successions varies considerably between individual interglacials. This is primarily due to species competition, distance to glacial refugia, and the specific climate conditions during individual interglacials as a consequence of specific orbital geometries (e.g., de Beaulieu et al., 2001; Tzedakis et al., 2001). The variations in tree compositions have important biostratigraphic consequences because they allow the assignment of discontinuous and fragmented pollen records to specific interglacials (e.g., de Beaulieu et al., 2001). Considering the above, we here analyse the pollen signals at Lake Ohrid in the context of the MIS 11 vegetation signature in Europe. Pollen records from both South and Central Europe show a unique tree composition for MIS 11; it is marked by a strong expansion of *Abies,* associated with a presence of *Pterocarya* and *Buxus* in comparison to younger interglacials (e.g., Desprat et al., 2005; Koutsodendris et al., 2010; Nitychoruk et al., 2005; Tzedakis et al., 2001). On the Iberian and Balkan Peninsulas MIS 11 is generally characterized by low abundances of *Carpinus* and *Fagus* (Desprat et al., 2005; Oliveira et al., 2016; Tzedakis et al., 2001).

Our new pollen record clearly bears the typical vegetation characteristics for MIS 11 as previously known from the Balkan Peninsula. Specifically, it is marked by high *Abies* percentages, a distinct phase of *Pterocarya* expansion, and low *Carpinus* and *Fagus* percentages (Fig. 3). However, a close comparison with the pollen records from Ioannina (470 m a.s.l.) and Tenaghi Philippon (40 m a.s.l.; Fig. 1) reveals a considerable regional heterogeneity across the Balkan Peninsula. The record from Ioannina (Tzedakis et al., 2001) exhibits higher percentages of thermophilous elements such as *Ulmus/Zelkova, Carpinus betulus*, and *Olea* than that from Lake Ohrid; in addition, *Buxus* is present and *Picea* is absent. The record from Tenaghi Philippon (Wijmstra and Smit, 1976) shows lower abundances of *Abies* and higher abundances of Mediterranean taxa (e.g., *Quercus ilex*, *Olea*, and *Phillyrea*) than Lake Ohrid; both *Buxus* and *Picea* are absent.

These differences suggest cooler climate conditions at Lake Ohrid during MIS 11 than at Ioannina and Tenaghi Philippon. We attribute this regional climate differentiation primarily to the higher-elevation setting of Lake Ohrid, which resulted in considerably lower temperatures in comparison to the lower-elevations site of Ioannina and Tenaghi Philippon. Consequently, although our new Lake Ohrid pollen record shows the typical vegetation characteristics of MIS 11, it also exhibits a distinct signature that can serve as a template for cooler, more inland settings of the Central Balkan Peninsula.

6.2. Insight into the Quaternary tree extirpation record of SE Europe

Because the Lake Ohrid area served as a refugium for European tree taxa during glacial periods (Lézine et al., 2010; Sadori et al., 2016), it is well suited to record the final disappearances of taxa that became extinct from Europe over the course of the Quaternary. The high tree-pollen diversity of the Lake Ohrid pollen record for MIS 11 (Figs. 3 and 6) suggests that many tree taxa managed to survive in this region during MIS 12, which was likely the coldest glacial of the entire Pleistocene (Naafs et al., 2014; Rohling et al., 2014). In the following, we use our pollen data from Lake Ohrid to shed light on the timing of the extinction of thermophilous taxa from Europe (i.e., *Carya*, *Cedrus*, *Parrotia*, *Pterocarya*, and *Tsuga*) and on the biogeographical constraints of currently present Tertiary relics (i.e., *Picea omorika*, *Zelkova*) in SE Europe.

An important prerequisite for identifying the last occurrences of pollen taxa is to be able to confidently exclude reworking from older strata or long-distance transport. Most of the taxa discussed here occur in abundances of more than a few grains in a considerable number of samples (i.e., *Carya*, *Fagus*, *Juglans*, *Pterocarya*, *Picea omorika*, and *Zelkova*); this occurrence pattern, together with the excellent preservation of the individual pollen grains, strongly reduces the likelihood of reworking. More caution is required for pollen taxa that appear only very sporadically in few samples of our record such as *Castanea*, *Cedrus*, *Parrotia*, *Tsuga,* and *Vitis*. The excellent preservation of the respective pollen grains in our material strongly suggests that their occurrence is not due to reworking from older strata; however, the presence of pollen grains of the conifers *Cedrus* and *Tsuga* should be interpreted with extreme caution because the morphology of their pollen grains makes them particularly prone to long-distance transport (Magri and Parra, 2002; Rousseau et al., 2006).

6.2.1. Extinct taxa

With respect to tree taxa that are extinct from Europe today, our results show that *Pterocarya* was a prominent rare element of the tree-pollen assemblages at Lake Ohrid during MIS 11 (Figs. 3 and 6). This is in agreement with other MIS 11 pollen records from across Europe (de Beaulieu et al., 2001; Desprat et al., 2005; Koutsodendris et al., 2010; Nitychoruk et al., 2005; Tzedakis et al., 2001). In younger interglacials, *Pterocarya* is only sporadically found on the Balkan (Tenaghi Philippon – Wijmstra and Smit, 1976;

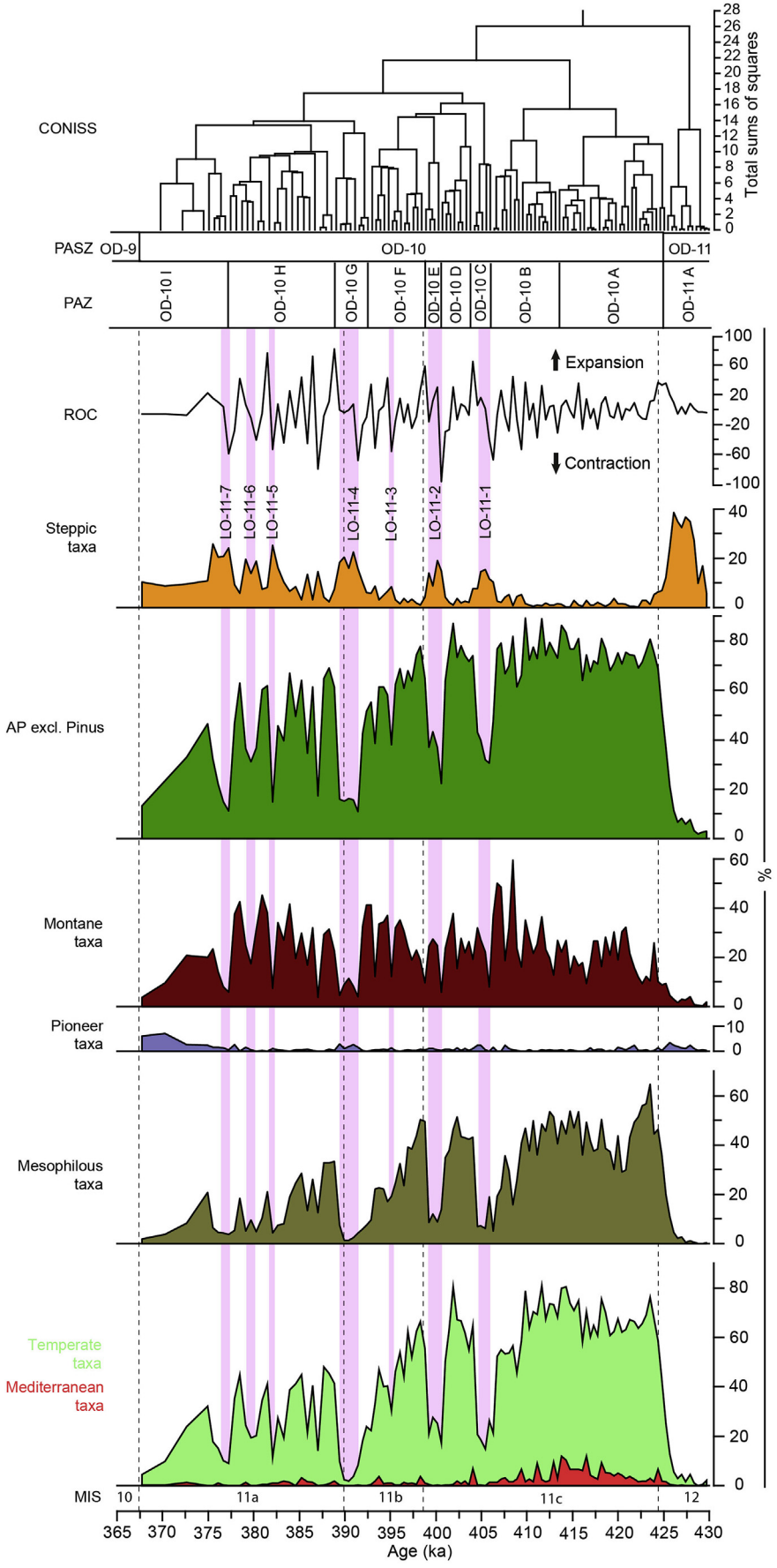
CONISS
Total sums of squares
PASZ OD-9 OD-10 OD-11
PAZ OD-10 I OD-10 H OD-10 G OD-10 F OD-10 E OD-10 D OD-10 C OD-10 B OD-10 A OD-11 A
ROC
Expansion
Contraction
LO-11-7 LO-11-6 LO-11-5 LO-11-4 LO-11-3 LO-11-2 LO-11-1
Steppic taxa
AP excl. Pinus
Montane taxa
Pioneer taxa
Mesophilous taxa
Temperate taxa
Mediterranean taxa
%
MIS 10 11a 11b 11c 12
Age (ka)

Table 1
Characteristics of major forest contraction events in the Lake Ohrid during MIS 11, and their suggested counterparts from the Iberian margin (IODP Site U1385) adapted from Oliveira et al. (2016). TANN: Mean annual temperature; MTCO: Mean temperature of the coldest month; PANN: mean annual precipitation.

Lake Ohrid (DEEP record)						Iberian margin (IODP Site U1385) (Oliveira et al., 2016)
Depth (mcd)	Age (ka)/Duration (kyrs)	Minimum AP (%) (number of samples)	Minimum TANN (^{0}C)	Minimum MTCO (^{0}C)	Minimum PANN (mm)	Event (Age) (ka)
LO-11-7 (158.67 −158.03)	377.9–375.5/2.4	11 (5)	4	−5	670	U1385-11-fe 8 (377.5)
LO-11-6 (159.31 −158.99)	380.3–379.1/1.2	31 (3)	4	−5	730	U1385-11-fe 7 (380.5)
LO-11-5 (160.11 −159.79)	383.3–382.1/1.2	15 (3)	2	−10	600	U1385-11-fe 6 (383)
LO-11-4 (162.51 −161.71)	391.9–389.4/2.5	11 (6)	2	−8	570	U1385-11-fe 5 (390)
LO-11-3 (163.79 −163.63)	396.0–395.1/0.9	38 (2)	3	−3	1000	U1385-11-fe 3 (396)
LO-11-2 (165.71 −165.07)	401.0–399.2/1.8	22 (5)	2	−7	620	U1385-11-fe 2 (399.5)
LO-11-1 (167.63 −167.00)	406.2–404.5/1.7	31 (5)	4	−9	550	U1385-11-fe 1 (408)

Kopais – Okuda et al., 2001) and Iberian (Desprat et al., 2009) Peninsulas during MIS 9. Moreover, in Central Italy it also occurs sporadically during MIS 7 (Valle di Castiglione – Follieri et al., 1988). Considering that *Pterocarya* requires mean annual and mean coldest month temperatures above 7.6 °C and −6.5 °C, respectively (Svenning, 2003), its exceptionally widespread distribution in Europe during MIS 11 delimits the minimum temperature background conditions for this interglacial across the continent; however, other factors such as competition with other tree taxa and migration patterns are also to be considered with regard to its spatiotemporal distribution.

Carya has been documented palynologically both at Tenaghi Philippon (Wijmstra and Smit, 1976) and in Central Italy (Magri et al., 2017) in interglacials younger than MIS 11 (i.e., during MIS 7 and 9, respectively). Interestingly, however, the presence of *Carya* appears to be discontinuous during Middle Pleistocene interglacials, and it has not yet been reported in Europe during MIS 11 (Magri et al., 2017). Because we can confidently exclude that the findings of *Carya* pollen in our record are due to reworking, the documentation of *Carya* at Lake Ohrid during MIS 11 (Fig. 6) indicates that this taxon may have grown continuously in Europe throughout the Middle Pleistocene. It also suggests that Lake Ohrid was one of the last refugial areas for this taxon on the European continent.

The available information for *Parrotia* and *Tsuga* suggests that both these taxa became extinct before MIS 11 in Europe, with the last sporadic appearances being during MIS 13 in Iberia, South and Central Italy (Combourieu-Nebout et al., 2015; Magri et al., 2017). Strikingly, the last documentation of *Parrotia* and *Tsuga* from SE Europe was much earlier, i.e., for MIS 17 on Rhodos Island (Joannin et al., 2007) and even MIS 19 at Tenaghi Philippon (van der Wiel and Wijmstra, 1987). Assuming that the findings of the respective pollen grains are not due to reworking, the much later documentation at Lake Ohrid (Fig. 6) suggests that *Parrotia* and *Tsuga* may have thrived in climatically and ecologically favorable pockets on the Balkan Peninsula for about 200–300 ka longer than previously known. However, further studies are required to confirm this hypothesis.

Finally, the sporadic occurrence of *Cedrus* pollen at Lake Ohrid during MIS 11 is in agreement with the presence of the taxon at several localities across the Mediterranean region, such as on the Iberian and Italian Peninsulas (Combourieu-Nebout et al., 2015; Magri et al., 2017), but also in the Balkans (i.e., Tenaghi Philippon; Wijmstra and Smit, 1976). Although the documentation of *Cedrus* at Lake Ohrid has to be seen with caution because of potential long-distance transport (Magri and Parra, 2002), our finding may point to a more widespread distribution of this conifer during MIS 11 in southern Europe than previously thought.

6.2.2. Tertiary relics

Pollen grains from two Tertiary relics are documented in the Lake Ohrid record for MIS 11, i.e., *Picea omorika* and *Zelkova* (Figs. 3 and 6). *Picea omorika* is currently endemic on the Balkan Peninsula, with the majority of the native populations occurring along the Drina River (Serbia/Bosnia-Herzegovina) over an area of only 4 km^2 (Nasri et al., 2007; San-Miguel-Ayanz et al., 2016). The taxon can occur in mixed and pure stands, but is usually suppressed by *Abies alba*, *Fagus* and *P. abies*, especially during times of enhanced climatic stress (Ballian et al., 2006). To date, the documentation of *P. omorika* during MIS 11 at Lake Ohrid represents the only unequivocal presence of the taxon in Europe during the Middle Pleistocene. It supports the hypothesis that the taxon has managed to survive through several glacial-interglacial cycles on the Balkan Peninsula. At the same time, however, its absence in other pollen records (e.g., Ioannina and Tenaghi Philippon) from the region suggests that Lake Ohrid must have comprised an area with sheltered topography and buffered stable microclimate for the taxon, hence acting as a 'cryptic' refugium (*sensu* Birks and Willis, 2008).

In contrast to *Picea omorika*, *Zelkova* does not currently grow in continental Europe, although it was common during MIS 11 at Ioannina (Tzedakis et al., 2001) and Tenaghi Philippon (Wijmstra and Smit, 1976); today, it only thrives on the islands of Sicily (Italy) and Crete (Greece) (Magri et al., 2017). Considering the high mean annual temperature required for *Zelkova* to grow (7.3 °C; Svenning, 2003), we attribute the disappearance of this taxon from the Balkan Peninsula to an overall cooling in this region over the

Fig. 4. Selected pollen groups and abrupt forest contractions during MIS 11 as identified in the Lake Ohrid DEEP core. Rate of change (ROC) of arboreal pollen (AP) % is indicative of abrupt forest expansion and contractions. The pollen assemblage zones (PAZ) are based on the CONISS dendrogram (Grimm, 1987), whereas the pollen assemblage superzones follow Sadori et al. (2016) for Lake Ohrid. Temperate taxa comprise all mesophilous deciduous and Mediterranean taxa as well as *Abies*, *Fagus*, *Ilex*, and *Taxus*; Mediterranean taxa comprise *Cistus*, *Fraxinus ornus*, *Olea*, *Phillyrea*, *Pistacia*, and *Quercus ilex*; montane taxa comprise *Abies*, *Betula*, *Fagus*, *Ilex*, *Picea*, and *Taxus*; pioneer taxa comprise *Ephedra fragilis* and *E. distachya* types, Ericaceae, *Hippophaë*, and *Juniperus*; steppic taxa comprise *Artemisia* and Chenopodiaceae.

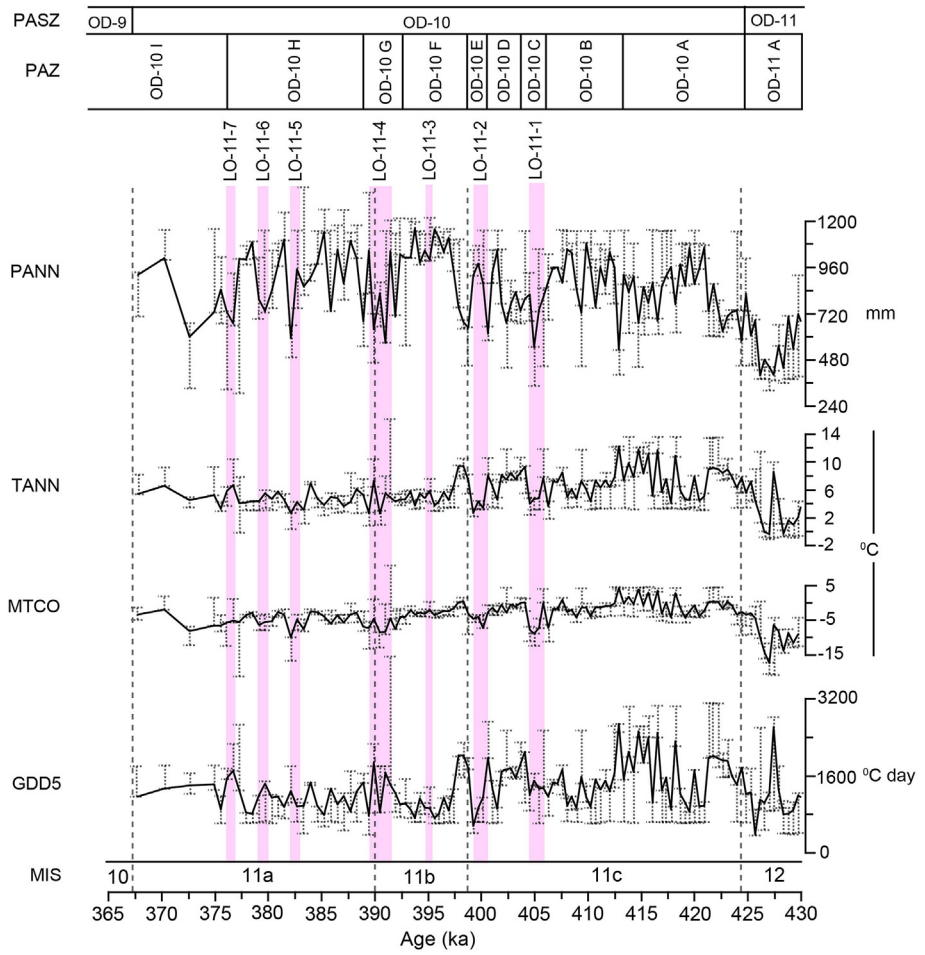

Fig. 5. Pollen-based paleoclimate reconstructions for MIS 11 at Lake Ohrid plotted against age. The dashed lines indicate the range covered by the closest five modern analogues. Pink bands represent the most prominent forest contraction events and black dashed lines MIS boundaries. (For interpretation of the references to color in this figure legend, the reader is referred to the Web version of this article.)

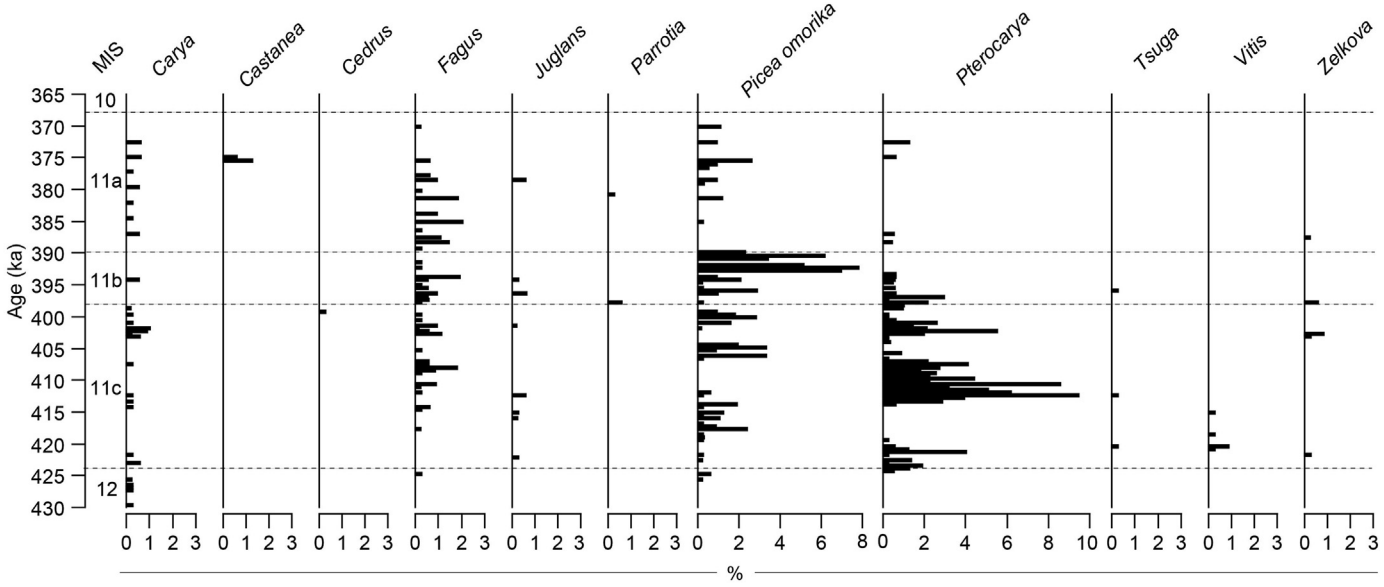

Fig. 6. Distribution of rare pollen taxa encountered in the Lake Ohrid record for MIS 11. MIS boundaries are indicated by black dashed lines.

past four glacial-interglacial cycles (Sadori et al., 2016; Tzedakis et al., 2006).

In summary, our results suggest that the natural arboreal vegetation on the Balkan Peninsula was more diverse during MIS 11 than today. In combination with the available pollen records across southern Europe (Combourieu-Nebout et al., 2015, Magri et al., 2017, and references therein), there is a tendency for later disappearances of rare trees at Lake Ohrid not only on Mediterranean-wide, but particularly also on Balkan-wide scales. This observation highlights the prominent role of Lake Ohrid as a refugium for thermophilous plants throughout the Quaternary. Future palynological analysis of sediments from Lake Ohrid – particularly from intervals younger than MIS 11 – and the integration of the results with available micro- and macrofloral records from the region will allow to significantly refine the timing and patterns connected to the demise of now extinct tree taxa from the Balkans and, by extension, from Europe.

6.3. Climatic implications of the Lake Ohrid pollen record

6.3.1. Long-term vegetation and climate variability

The shift from an open environment with steppe vegetation to closed forests dominated by temperate tree taxa at the onset of MIS 11c (Fig. 4) suggests a transition towards warmer and wetter climate conditions. Based on our quantitative climate estimates, the transition to MIS 11c is associated with pronounced increases in TANN (by 7 °C), MTCO (15 °C) and PANN (150 mm; Fig. 5). Further support for warming at that time comes from the increases in total organic and inorganic carbon contents in the Lake Ohrid cores (Fig. 7; Francke et al., 2016). They indicate enhanced primary productivity and higher water temperatures in Lake Ohrid during spring and summer, as well as stronger chemical weathering in the catchment due to warmer conditions and thus a higher input of Ca^{2+} and HCO_3^- into the lake (Francke et al., 2016). The development of closed forests around Lake Ohrid under a warmer/wetter climate than during MIS 12 is further corroborated by XRF data from the DEEP Site; they show a decrease of K values concurrent with the temperate taxa increase during MIS 11c (Fig. 7), reflecting reduced erosion in the lake catchment as a result of soil stabilization (Francke et al., 2016). This suggests a fast spreading of forests around Lake Ohrid with the onset of warmer conditions, a scenario that is further supported by the presence of trees throughout MIS 12 in the catchment area of the lake (Sadori et al., 2016).

The evaluation of the pollen data indicates that MIS 11c is the warmest interval of MIS 11. The percentages for mesophilous and Mediterranean taxa peak during that time, reaching ~65% at 423 ka and 12% at 414 ka, respectively (Fig. 4). This interpretation is further supported by the presence of thermophilous taxa including *Quercus ilex* type, *Phillyrea, Fraxinus excelsior* type, and *F. ornus* (Fig. 3), all of which require warm and dry summers and mild winters to grow (San-Miguel-Ayanz et al., 2016). Other sensitive climate indicators are also sporadically present during MIS 11c; these include *Hedera*, which cannot bloom in areas with a mean January temperature below −2 °C (Iversen, 1944; Müller et al., 2005, and references therein), and *Taxus*, which can tolerate average temperatures of the coldest month as low as −5 °C and is known to favor high-precipitation settings (San-Miguel-Ayanz et al., 2016; Sykes et al., 1996). In line with these taxon-specific climate requirements, our pollen-based temperature estimates suggest that MIS 11c was characterized by relatively high TANN (mean: 7.1 °C) and MTCO (mean: −1.5 °C) values; within MIS 11c, the warmest conditions prevail between 415 and 412 ka as documented by even higher TANN values (mean: 9.5 °C) and likely frost-free winters (mean MTCO: 1.5 °C; Fig. 5). This finding is in agreement with TIC values that indicate highest spring and summer temperatures in Lake Ohrid at that time (Francke et al., 2016, Fig. 7). It gains further support through oxygen-isotope data from endogenic calcite in the DEEP cores; these data show high values indicative of enhanced evaporation under warm and/or dry conditions during MIS 11c, with a peak at 412–410 ka (Lacey et al., 2016, Fig. 7).

Based on the above, all biotic and abiotic proxy signals from Lake Ohrid consistently indicate warm climate conditions during MIS 11c, with peak warmth being reached at 415–412 ka, i.e., ~9–12 ka after the onset of the interglacial. This is in broad agreement with regional and global proxy records. Deuterium-based temperature reconstructions from Antarctica show a continuously increasing temperature during MIS 11c (Jouzel et al., 2007). For the terrestrial realm of the Northern Hemisphere, palynological evidence from ODP Site 646 in the North Atlantic documents the existence of boreal forests on Greenland during the youngest interval of MIS 11c (de Vernal and Hillaire-Marcel, 2008), a period associated with the collapse of the Greenland ice sheet (Reyes et al., 2014). This finding from the northern high latitudes is in agreement with further proxy data from the Siberian Arctic; for Lake El'gygytgyn, pollen-based temperature reconstructions and the XRF-based Si/Ti ratio (Fig. 7), which is an indicator for lake productivity, suggest that the youngest interval of MIS 11c exhibited the highest temperatures of the past 1 Ma (Melles et al., 2012).

Our temperature inferences for Lake Ohrid are also corroborated by marine proxy records. Foraminifera- and alkenone-based sea-surface temperature (SST) reconstructions from the central North Atlantic (IODP Site U1313; Stein et al., 2009) and the Iberian margin (Rodrigues et al., 2011; Voelker et al., 2010) correlate well within the uncertainties of the age models with the temperature increase derived from the palynological record for Lake Ohrid (Fig. 7). Moreover, the timing of peak warmth ~9–12 ka after the onset of MIS 11c as documented for Lake Ohrid agrees well with sea-level reconstructions that indicate an up to 20 ka long deglaciation period during MIS 11c and peak warmth during the younger parts of MIS 11c (Raymo and Mitrovica, 2012; Rohling et al., 2010). In light of these comparisons, the climate-proxy data from Lake Ohrid record sensitively both the high- and mid-latitude climate dynamics during MIS 11c.

An exceptional characteristic of the MIS 11c interglacial is that it spans two insolation peaks (e.g., Berger, 1978; Yin and Berger, 2015). The impact of insolation variability on the climate dynamics during MIS 11c is documented in the atmospheric CO_2 (Lüthi et al., 2008) and CH_4 (Loulergue et al., 2008, Fig. 7) records from Antarctic ice cores; they follow a characteristic 'M' pattern denoting a two-time increase and decrease. This pattern has also been captured by several marine (i.e., foraminifera- and alkenone-based SST) records from the North Atlantic (Rodrigues et al., 2011; Stein et al., 2009) and terrestrial records from the Iberian margin (Desprat et al., 2005; Tzedakis et al., 2009), suggesting a coeval response to global climate change (Fig. 7).

Our new palynological data from Lake Ohrid also document this characteristic climate feature of MIS 11c. Specifically, the percentages of the temperate taxa increase after the onset of the interglacial at 424 ka and remain high until 421 ka, then slightly decrease until 416 ka, and subsequently increase to maximum values between 415 and 409 ka (Fig. 7). These changes, which generally follow the insolation curve, are also in good agreement with the CH_4 record (Loulergue et al., 2008, Fig. 7). The 'M' pattern in Lake Ohrid also emerges from the percentages of mesophilous taxa (Fig. 4), and it is also mirrored in the TANN and MTCO estimates that show lower temperatures from 421 to 416 ka between two intervals with higher temperatures from 424 to 421 ka and from 415 to 409 ka, respectively (Fig. 5). Interestingly, the percentage decrease in temperate taxa between 420 and 416 ka appears less pronounced at Lake Ohrid than off Iberia (core MD01-

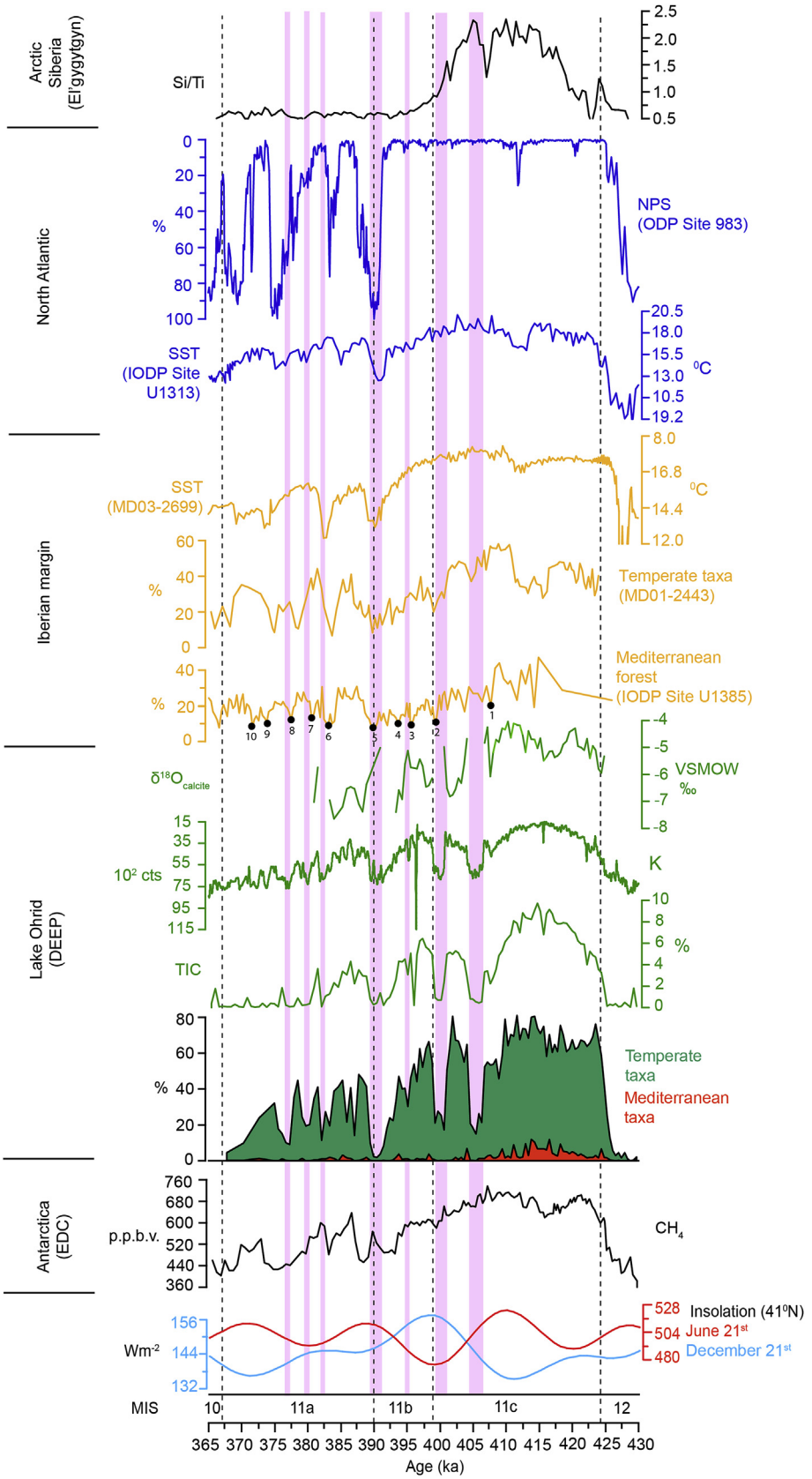

Fig. 7. Selected palynological data from the Lake Ohrid DEEP core plotted against insolation at 41 °N (Berger, 1978), CH_4 concentrations from Antarctic ice cores (EDC; Loulergue et al., 2008), total inorganic carbon (TIC), XRF-based potassium (K) counts (Francke et al., 2016) and oxygen isotopes on endogenic calcite ($\delta^{18}O_{calcite}$; Lacey et al., 2016) from the DEEP core, Mediterranean forest percentages from IODP Site U1385 (Oliveira et al., 2016), temperate taxa percentages from core MD01-2443 (Tzedakis et al., 2009), alkenone-based sea-surface temperature (SST) reconstructions from core MD03-2699 (Rodrigues et al., 2011) and IODP Site U1313 (Stein et al., 2009), *Neogloboquadrina pachyderma* sinistral (NPS) percentages from ODP Site 983 (Barker et al., 2015), and Si/Ti ratio from Lake El'gygytgyn (Melles et al., 2012). Note reversed axes of the potassium (K) and NPS records. Numbering in the pollen record from IODP Site U1385 represents abrupt forest setbacks on Iberia (Oliveira et al., 2016; compare also Table 1). Pink bands represent the most prominent forest contraction events in Lake Ohrid, and black dashed lines indicate MIS boundaries.

2443; Tzedakis et al., 2009). In addition, the respective percentage decrease in core MD01-2443 occurs ~4 ka later during MIS 11c (i.e., 416–411 ka) than in Lake Ohrid, thereby post-dating the decrease in atmospheric CH_4 (compare Fig. 7). While these temporal offsets are most likely due to age-model uncertainties, we consider it improbable that a temperature difference between the two localities may have been responsible for the different vegetation signatures given that the two records represent similar latitudes (Fig. 1) and hence receive similar insolation. Instead, we attribute the subtle decline of the temperate taxa at Lake Ohrid to persistently high water availability during the insolation minimum on the SW Balkan Peninsula. Higher humidity in combination with decreasing insolation would promote the growth of temperate taxa such as *Abies* at the expense of deciduous *Quercus*, as documented in our pollen record (Fig. 3). Our hypothesis is further supported by our pollen-based climate estimates that show an increase in PANN to above 900 mm for this interval (Fig. 5).

The MIS 11b and 11a intervals (398–377 ka) show a general decrease in the percentages of temperate and Mediterranean taxa, while montane taxa and steppic elements (*Artemisia*, Chenopodiaceae) increase gradually (Fig. 4). In our climate estimates, this vegetation shift is reflected in a GDD5 decrease from a mean of ~1550 °C days during MIS 11c to ~1100 °C days during MIS 11b–a (Fig. 5), which in combination with the high moisture availability (average PANN: ~900 mm) suggests a transition from temperate deciduous to cold mixed forests (Prentice et al., 1992). Similarly, our temperature estimates also document lower TANN and MTCO values than during MIS 11c (Fig. 5). Independent geochemical evidence (TIC and $\delta^{18}O_{calcite}$) from the Lake Ohrid DEEP core (Francke et al., 2016; Lacey et al., 2016) also indicates a shift towards cooler conditions (Fig. 7).

On a regional scale, cooling at Lake Ohrid during MIS 11b-a is in agreement with the information from pollen records across the Mediterranean region such as from Tenaghi Philippon (Tzedakis et al., 2006; Wijmstra and Smit, 1976), Ioannina (Tzedakis et al., 2001), Praclaux (Reille et al., 2000), and Iberia (Desprat et al., 2005; Oliveira et al., 2016; Tzedakis et al., 2009). They consistently show an expansion of open vegetation communities at the expense of temperate forests. It is further corroborated by SST records from the North Atlantic (Rodrigues et al., 2011; Stein et al., 2009; Voelker et al., 2010) and Antarctic ice-core records (Jouzel et al., 2007; Loulergue et al., 2008) (Fig. 7).

6.3.2. Millennial-scale vegetation and climate variability

6.3.2.1. The LO-11-1 forest contraction (406.2–404.5 ka) during MIS 11c. Interrupting the predominantly stable climate conditions registered for MIS 11c, our pollen data document a pronounced forest contraction event, i.e., LO-11-1, between 406.2 and 404.5 ka that merits special attention. This vegetation setback occurs within full interglacial conditions, ~7 ka before the end of MIS 11c that itself occurred during a summer insolation minimum at ~398 ka (Fig. 7). It is characterized by a strong tree-pollen decrease from ~406 ka onwards that is mainly due to a percentage decline of temperate and Mediterranean taxa, and lasts for ~1.7 kyrs (Fig. 7). Our pollen-based climate estimates indicate that the forest contraction is associated with decreases in both temperature and precipitation; in particular, TANN decreases from ~8 to ~4 °C, MTCO from 1 to −9 °C, and PANN from 960 to ~550 mm (Table 1; Fig. 5). An impact of this event is also documented for the aquatic ecosystem of Lake Ohrid: Synchronously with temperate taxa percentages, TIC and TOC decrease, indicating lower water temperature and primary productivity, respectively (Francke et al., 2016, Fig. 7).

The strong imprint of the LO-11-1 event on both the catchment area and the limnic ecosystem of Lake Ohrid during full interglacial conditions raises the question about its trigger mechanism. A first step towards resolving this issue is to constrain the spatial distribution of the event. Accepting minor, inevitable offsets in the timing of potentially equivalent events in other archives as they arise from age-model uncertainties, an impact of the LO-11-1 event on vegetation is clearly documented in pollen records from the Iberian margin. Transient forest contractions are recorded in core MD01-2443 at ~406 ka (based on the chronology of core MD01-2443; Tzedakis et al., 2009, Fig. 7) and at IODP Site U1385 (event U1385–11–fe1 at ~408 ka according to the Site U1385 chronology; Oliveira et al., 2016) (Table 1; Fig. 7). Although the LO-11-1 event is not registered in the available low-resolution pollen records from Southern Europe (Praclaux – de Beaulieu et al., 2001; Tenaghi Philippon – Wijmstra and Smit, 1976; Ioannina – Tzedakis et al., 2001), the observation that it has affected terrestrial ecosystems both on the Balkan and the Iberian Peninsulas testifies to its supraregional distribution. In their study from the Iberian margin, Oliveira et al. (2016) have examined the possibility that this event may represent the 'Older Holsteinian Oscillation' (OHO), a prominent, short-lived cooling event that affected terrestrial ecosystems in Europe north of 50° latitude at ~408 ka (±0.5 ka; Koutsodendris et al., 2012). Considering that the duration of the OHO in Europe north of the 50th parallel was only 220 years based on varve counting (Koutsodendris et al., 2011, 2012), it appears unlikely that the event that impacted the Balkan and Iberian peninsulas for ~1–2 kyrs and the OHO are identical.

Unfortunately, the floating chronologies of the pollen records north of the Alps in Central Europe (Koutsodendris et al., 2012, and references therein) preclude direct correlation with pollen records from southern Europe. However, additional evidence for a cooling event at ~406–404 ka comes from $\delta^{18}O_{carbonate}$ data from the Pianico paleolake (Southern Alps; Fig. 1). Pianico represents a 15.5-ka-long, varved archive (Mangili et al., 2007); its floating chronology has been tied to a tephra layer with an age of 393 ± 12 ka (Brauer et al., 2007a), although there is still an ongoing debate on the age of the succession (compare Brauer et al., 2007b; Pinti et al., 2001; Roulleau et al., 2009). If the chronology proposed by Brauer et al. (2007a) is correct, the $\delta^{18}O_{carbonate}$ record from Pianico shows an abrupt, cooling-induced shift towards lighter values at ~405 ka (Mangili et al., 2007). Based on varve counting, this event lasted for 780 years (Mangili et al., 2007), and it appears to have been associated with an abrupt vegetation shift from broad-leaved trees to conifers as shown by pollen data (Rossi, 2003).

Beyond southern Europe, there is further evidence from Siberia that terrestrial ecosystems were affected by short-term cooling at ~405 ka. A high-resolution pollen record from Lake Baikal shows a transient expansion of cold-tolerant taxa (i.e., *Pinus pumila* and *P. sibirica*) at 405 ka, indicating a prevalence of cooler conditions for ~1 kyr (Prokopenko et al., 2010). Sediment geochemical data from Lake El'gygytgyn (Arctic Siberia) also suggest a transient shift to lower lake productivity under cooler climate conditions; the Si/Ti ratio strongly decreases at ~407 ka and remains low for ~2 kyrs (Melles et al., 2012, Fig. 7). Although this shift seems to have occurred ~1 ka earlier than at Lake Ohrid based on the available age models from both sites, it is noteworthy that the shift observed at Lake El'gygytgyn is the only one of its kind over the course of MIS 11c at that site (Melles et al., 2012). We therefore posit that this event may in fact be synchronous with the LO-11-1 event at Lake Ohrid.

In contrast to the terrestrial realm, which appears to have been impacted by climate change at ~405 ka across parts of Eurasia, no sign of synchronous climate change has yet emerged from marine proxy records. In particular, it is puzzling that neither the surface-water datasets available from the Iberian margin (Oliveira et al., 2016; Rodrigues et al., 2011) nor from the central (Stein et al.,

2009) and northern North Atlantic (Barker et al., 2015; Kandiano et al., 2017) show any indication of cooling at ~405 ka, although their temporal resolution is high enough to register such a signal (Fig. 7). As an explanation for this apparent discrepancy between marine and terrestrial records, it has been suggested that the U1385-11-fe1 event may have been associated with drier rather than cooler conditions, perhaps related to a persistent positive mode of the North Atlantic Oscillation (NAO; Oliveira et al., 2016). Associated with the relative strengths of the Azores and Iceland pressure systems, the NAO affects the position of the Westerlies and hence precipitation variability across Europe (e.g., Wanner et al., 2001). A potential connection of the U1385-11-fe1 event, and hence its equivalent LO-11-1 in Lake Ohrid, to NAO dynamics gains further support considering that NAO variability was a persistent feature of European climate during MIS 11 (Kandiano et al., 2012; Koutsodendris et al., 2011). A close inspection of the pollen data from Lake Ohrid shows that the event occurred during a time when conifer forests with *Picea abies* and *Abies* dominated the catchment area of the lake (Fig. 3); the percentage increases of these taxa at the expense of deciduous trees started at ~409 ka. Although *Picea* and *Abies* can tolerate cold and frosty conditions, they are sensitive to water deficit (e.g., San-Miguel-Ayanz et al., 2016; Sykes et al., 1996). Therefore, the reduced percentages of these taxa at Lake Ohrid at ~405 ka (Fig. 3) support a scenario of decreasing water availability beyond a critical threshold along with climatic cooling as the underlying mechanism for the LO-11-1 event.

In summary, our new pollen data from Lake Ohrid provide evidence for a strong climatic event that occurred ~7 ka before the end of MIS 11c (*sensu* Tzedakis et al., 2001) and ~15 ka before the onset of ice-rafted debris (IRD) deposition in the North Atlantic during MIS 11 (Barker et al., 2015; Martrat et al., 2007; Oppo et al., 1998). Comparison with other proxy records from the Northern Hemisphere that cover the respective interval in sufficiently high resolution suggests that the event is not expressed in the marine realm. This means that millennial-scale variability during MIS 11 is registered earlier in terrestrial settings than in the marine realm because the combination of dry and cold conditions left a clear imprint on vegetation. By extension, millennial-scale variability during MIS 11 existed during periods of low ice volume.

It has been shown previously that forest contractions under low-ice-volume conditions that are not followed by forest recovery are a common feature of interglacials younger than MIS 11 (Tzedakis et al., 2004). Thus, such millennial-scale events appear to have been responsible for a potentially 'premature' ending of interglacials in the terrestrial realm (Tzedakis et al., 2004). In contrast, the pollen record from Lake Ohrid provides evidence for a re-expansion of temperate forests following the LO-11-1 event (Fig. 7). This is in agreement with the pollen data from the Iberian margin, which also document the development of temperate forests subsequently to the event until the insolation minimum at ~398 ka (Desprat et al., 2005; Tzedakis et al., 2009, Fig. 7). The forest recovery can be attributed to the prolonged warm conditions in the Northern Hemisphere during MIS 11c (e.g., de Vernal and Hillaire-Marcel, 2008; Melles et al., 2012; Prokopenko et al., 2010), perhaps associated with a persistent vigorous circulation in the North Atlantic (e.g., Barker et al., 2015; Koutsodendris et al., 2014; Martrat et al., 2007; Voelker et al., 2010).

6.3.2.2. Additional forest contractions. The end of MIS 11c in the Lake Ohrid pollen record is marked by a strong forest contraction at 401.0–399.2 ka (here termed LO-11-2). Our quantitative climate estimates yield TANN and MTCO minima of 2 and -7 °C, respectively, and PANN declined to ~620 mm during this event (Table 1; Fig. 5). Other proxy data from the Lake Ohrid cores also suggest a coeval marked cooling for the aquatic environment of the lake; in particular, TOC and TIC values declined strongly. At the same time, soil erosion in the catchment area of the lake was enhanced as suggested by an increase in the K content of the sediment (Francke et al., 2016, Fig. 7). The timing of the LO-11-2 event is synchronous with that of the summer insolation minimum (Fig. 7), which is widely considered to have terminated the interglacial climate conditions of MIS 11c (e.g., Müller and Pross, 2007; Tzedakis et al., 2009). Accordingly, the cause for this event is connected to Northern Hemisphere cooling as a consequence of orbital forcing.

In concert with previously published sedimentological and geochemical information from Lake Ohrid, our palynological data provide evidence for considerable sub-millennial- to millennial-scale variability superimposed on the gradual cooling trend during MIS 11b and 11a. This is documented by the highly fluctuating percentages of AP, temperate taxa and steppic elements (Fig. 4) as well as the variability in TIC values and K content (Fig. 7; Francke et al., 2016). Although such millennial-scale variability has been previously documented in terrestrial records from southern Europe, including Tenaghi Philippon (Tzedakis et al., 2006; Wijmstra and Smit, 1976) and the Iberian margin (Oliveira et al., 2016; Tzedakis et al., 2009), the high temporal resolution of our Lake Ohrid record allows to further refine the nature and tempo of this variability in the Eastern Mediterranean region. Specifically, our data document at least five, 0.9 to 2.5-kyrs-long forest contractions at 396.0–395.1, 391.9–389.4, 383.3–382.1, 380.3–379.1, and 377.9–375.5 ka (LO-11-3 to LO-11-7; Table 1). Comparable forest contractions are also recorded in the pollen data from IODP Site U1385 off Iberia (Oliveira et al., 2016, Table 1), suggesting that millennial-scale climate variability is a persistent feature of terrestrial records during MIS 11b and 11a across Southern Europe.

Interestingly, however, not all forest contractions recorded at Lake Ohrid and the Iberian margin have counterparts in marine proxy records. Foraminifera- and alkenone-based SST reconstructions from the Central North Atlantic (Stein et al., 2009) and the Iberian margin (Martrat et al., 2007; Oliveira et al., 2016; Rodrigues et al., 2011) show three prominent cooling events centered at ~390, ~382 and ~377 ka, as do *Neogloboquadrina pachyderma* sinistral and IRD records at IODP Site 983 in the northern North Atlantic (Barker et al., 2015, Fig. 7). For these three events, marine proxy data indicate a slowdown of the Atlantic meridional overturning circulation associated with the expansion of ice sheets in the high-latitude Northern Hemisphere (Barker et al., 2015; Martrat et al., 2007; Stein et al., 2009) and cooling of the European continent (Desprat et al., 2005; Oliveira et al., 2016; Tzedakis et al., 2009). Concomitant cooling pulses in continental Europe is also suggested by our quantitative climate estimates for Lake Ohrid, which yield very low MTCO (−8, −10 and −5 °C, respectively) and PANN (570, 600, 670 mm, respectively) for the LO-11-4, LO-11-5 and LO-11-7 events (Table 1; Fig. 5).

The other two events at ~395 and ~380 ka (i.e., LO-11-3 and LO-11-6) have yet remained unknown in the marine realm. Importantly, they are documented in the pollen record from Site U1385, but not in the marine proxy data from the same core (Oliveira et al., 2016). As already touched upon in Section 6.3.2.1, this discrepancy has given rise to the hypothesis that these events were caused primarily by drier conditions related to a persistently positive NAO mode, which reduced the moisture availability on Iberia, but had only very limited impact on oceanic surface-water temperatures (Oliveira et al., 2016). The pollen-based climate estimates from Lake Ohrid, however, document only a minor precipitation decrease and a still relatively high moisture availability on the SW Balkan Peninsula during these events (Table 1; Fig. 5). Specifically, the LO-11-3 event at ~395 ka and the LO-11-6 event at ~380 ka are associated with PANN values of ~1000 mm and ~730 mm, respectively (Table 1). The scenario of drier conditions in Iberia and wetter

conditions in the Balkans during these forest-contraction events suggests the development of a see-saw pattern in precipitation between the western and eastern Mediterranean regions. An inversed precipitation pattern across the Mediterranean region (i.e., wet Iberia and dry Balkan peninsulas) has been documented for the Little Ice Age (LIA) during the last millennium based on instrumental and paleoclimatic data (e.g., Corella et al., 2014; Koutsodendris et al., 2017; Roberts et al., 2012). Although the boundary conditions and the moisture distribution during the LIA were different from those of MIS 11b-a, the precipitation contrast between SW and SE Europe during that time points to persistent atmospheric circulation patterns as the underlying cause for the LO-11-3 and LO-11-6 climatic events. Further paleoclimate data from regions sensitive to such atmospheric patterns are needed to confirm this hypothesis.

7. Conclusions

A new, centennial-scale-resolution palynological record has been generated across MIS 11 from the DEEP Site in Lake Ohrid (SW Balkan Peninsula). Augmented by quantitative pollen-based climate estimates, it provides new insight into the characteristics of short-term climate variability during MIS 11 in SE Europe. Our data suggest that in the Lake Ohrid region MIS 11 can be subdivided into two intervals: (i) MIS 11c, which was climatically relatively stable and marks an interval of full interglacial conditions from 424 to 398 ka, and (ii) MIS 11b and 11a (398–367 ka), which are characterized by general cooling and exhibit considerable millennial-scale variability. The new Lake Ohrid pollen record also documents a climatically driven forest contraction within full interglacial conditions, which based on the resolution of our data lasted for ~1.7 kyrs (~406.2–404.5 ka). This event is related to a combination of decreasing temperatures and water availability attributed to persisting atmospheric circulation patterns. This observation suggests that the onset of millennial-scale climate variability during MIS 11 pre-dates the first strong IRD event in the North Atlantic by ~15 ka.

In addition, our pollen record exhibits a series of forest contractions that have been also previously documented in pollen records from the Iberian margin. The most prominent of our events at ~399 occurs during the summer insolation minimum at the end of MIS 11c, suggesting a connection to orbital forcing as the underlying trigger mechanism. In addition, three events centered at ~390, ~382.5, and ~376.5 ka have a strong imprint in marine records from the North Atlantic, suggesting an AMOC slowdown as their trigger mechanism. Notably, two forest contractions at ~395 and ~380 ka that have been also registered in pollen records off Iberia, have no counterparts in the marine proxy records from the North Atlantic. It appears likely that these forest contractions have been caused by changes in atmospheric circulation, which affected water availability across the Mediterranean region.

Finally, our results confirm earlier studies suggesting that the Lake Ohrid area has acted as a tree refugium during the Middle Pleistocene. The presence of several tree taxa during MIS 11 that are now extinct from continental Europe (i.e., *Carya*, *Cedrus*, *Parrotia*, *Pterocarya*, and *Tsuga*) as well as the presence of Tertiary relics (i.e., *Picea omorika* and *Zelkova*) support the notion that forest diversity at Lake Ohrid was higher during this interglacial than during the Holocene, and that the area has experienced later tree extirpations than other localities across the Mediterranean region.

Acknowledgements

We thank T. Donders, T. Fischer, K. Panagiotopoulos, L. Sadori, and the members of the palynological team of the Lake Ohrid drilling project for fruitful discussions on vegetation dynamics on the Balkan Peninsula. We are also grateful to A. Bahr, O. Friedrich, and P. Vakhrameeva for discussions, D. Oliveira for sharing pollen data from IODP Site U1385, and S. Liner for sample processing. The constructive comments of two anonymous reviewers have improved this manuscript. Financial support by the Deutsche Forschungsgemeinschaft (DFG; grants KO4960/1 and WA2109/13) is gratefully acknowledged. This is an ISEM contribution n° 2017-299.

Appendix A. Supplementary data

Supplementary data related to this article can be found at https://doi.org/10.1016/j.quascirev.2018.04.014.

References

Andersen, S.T., 1994. History of the terrestrial environment in the Quaternary of Denmark. Bull. Geol. Soc. Den. 41, 219–228.
Ballian, D., Longauer, R., Mikić, T., Paule, L., Kajba, D., Gömöry, D., 2006. Genetic structure of a rare European conifer, Serbian spruce (*Picea omorika* (Panč.) Purk. Plant Systemat. Evol. 260, 53–63.
Barberi, F., Buonasorte, G., Cioni, R., Fiordelisi, A., Foresi, L., Iaccarion, S., Laurenzi, M.A., Sbrana, A., Vernia, I., Villa, I.M., 1994. Plio-Pleistocene geological evolution of the geothermal area of Tuscany and Latium. Mem. Descr.lla Carta Geol. Italia 49, 77–134.
Barker, S., Chen, J., Gong, X., Jonkers, L., Knorr, G., Thornalley, D., 2015. Icebergs not the trigger for North Atlantic cold events. Nature 520, 333–336.
Berger, A., Guiot, J., Kukla, G., Pestiaux, P., 1981. Long-term variations of monthly insolation as related to climatic changes. Geol. Rundsch. 70, 748–758.
Berger, A., 1978. Long-term variations of daily insolation and Quaternary climatic changes. J. Atmos. Sci. 35, 2362–2367.
Bertini, A., Sadori, L., Combourieu-Nebout, N., Donders, T.H., Kouli, K., Koutsodendris, A., Joannin, S., Masi, A., Mercuri, A.M., Panagiotopoulos, K., Peyron, O., Sinopoli, G., Torri, P., Zanchetta, G., Wagner, B., 2016. All together now: an international palynological team documents vegetation and climate changes during the last 500 kyr at Lake Ohrid (SE Europe). Alpine Mediterr. Quat. 29, 201–210.
Bigazzi, G., Bonadonna, F., Cioni, R., Leone, G., Sbrana, A., Zanchetta, G., 1994. Nuovi dati geochimici, petrografici e geocronologici su alcune cineriti Plio-Pleistoceniche del Lazio e della Toscana. Mem. Descr.lla Carta Geol. Italia 49, 135–150.
Billups, K., Chaisson, W., Worsnopp, M., Thunell, R., 2004. Millennial-scale fluctuations in subtropical northwestern Atlantic surface ocean hydrography during the mid-Pleistocene. Paleoceanography 19. PA2017.
Birks, H.J., Birks, H.H., 2004. Paleoecology. The rise and fall of forests. Science 305, 484–485.
Birks, H.J.B., Willis, K.J., 2008. Alpines, trees, and refugia in Europe. Plant Ecol. Divers. 1, 147–160.
Blockley, S.P.E., Pyne-O'Donnell, S.D.F., Lowe, J.J., Matthews, I.P., Stone, A., Pollard, A.M., Turney, C.S.M., Molyneux, E.G., 2005. A new and less destructive laboratory procedure for the physical separation of distal glass tephra shards from sediments. Quat. Sci. Rev. 24, 1952–1960.
Bosmans, J.H.C., Drijfhout, S.S., Tuenter, E., Hilgen, F.J., Lourens, L.J., Rohling, E.J., 2015. Precession and obliquity forcing of the freshwater budget over the Mediterranean. Quat. Sci. Rev. 123, 16–30.
Brauer, A., Wulf, S., Mangili, C., Moscariello, A., 2007a. Tephrochronological dating of varved interglacial lake deposits from Pianico-Sèllere (Southern Alps, Italy) to around 400 ka. J. Quat. Sci. 22, 85–96.
Brauer, A., Wulf, S., Mangili, C., Appelt, O., Moscariello, A., 2007b. Reply: tephrochronological dating of varved interglacial lake deposits from Pianico-Sèllere (Southern Alps, Italy) to around 400 ka. J. Quat. Sci. 22, 415–418.
Candy, I., Schreve, D.C., Sherriff, J., Tye, G.J., 2014. Marine Isotope Stage 11: palaeoclimates, palaeoenvironments and its role as an analogue for the current interglacial. Earth Sci. Rev. 128, 18–51.
Čarni, A., Matevski, V., 2015. Impact of climate change on mountain flora and vegetation in the Republic of Macedonia (Central part of the Balkan Peninsula). In: Öztürk, M., Hakeem, K., Faridah-Hanum, I., Efe, R. (Eds.), Climate Change Impacts on High-altitude Ecosystems. Springer International Publishing, pp. 189–213.
Cioni, R., Sbrana, A., Bertagnini, A., Buonasorte, G., Landi, P., Rossi, U., Salvati, L., 1987. Tephrostratigraphic correlations in the vulsini, Vico and sabatini volcanic successions. Period. Mineral. 56, 137–155.
Combourieu-Nebout, N., Bertini, A., Russo-Ermolli, E., Peyron, O., Klotz, S., Montade, V., Fauquette, S., Allen, J., Fusco, F., Goring, S., Huntley, B., Joannin, S., Lebreton, V., Magri, D., Martinetto, E., Orain, R., Sadori, L., 2015. Climate changes in the central Mediterranean and Italian vegetation dynamics since the Pliocene. Rev. Palaeobot. Palynol. 218, 127–147.
Corella, J.P., Benito, G., Rodriguez-Lloveras, X., Brauer, A., Valero-Garcés, B.L., 2014. Annually resolved lake record of extreme hydro-meteorological events since AD 1347 in NE Iberian Peninsula. Quat. Sci. Rev. 93, 77–90.

de Beaulieu, J.-L., Andrieu-Ponel, V., Reille, M., Grüger, E., Tzedakis, C., Svobodova, H., 2001. An attempt at correlation between the Velay pollen sequence and the Middle Pleistocene stratigraphy from central Europe. Quat. Sci. Rev. 20, 1593–1602.
de Vernal, A., Hillaire-Marcel, C., 2008. Natural variability of Greenland climate, vegetation, and ice volume during the past million years. Science 320, 1622–1625.
Desprat, S., Sánchez Goñi, M.F., Turon, J.L., McManus, J.F., Loutre, M.F., Duprat, J., Malaizé, B., Peyron, O., Peypouquet, J.P., 2005. Is vegetation responsible for glacial inception during periods of muted insolation changes? Quat. Sci. Rev. 24, 1361–1374.
Desprat, S., Sánchez Goñi, M.F., McManus, J., Duprat, J., Cortijo, E., 2009. Millennial-scale climatic variability between 340 000 and 270 000 years ago in SW Europe: evidence from a NW Iberian margin pollen sequence. Clim. Past 5, 53–72.
Fawcett, P.J., Werne, J.P., Anderson, R.S., Heikoop, J.M., Brown, E.T., Berke, M.A., Smith, S.J., Goff, F., Donohoo-Hurley, L., Cisneros-Dozal, L.M., Schouten, S., Sinninghe Damste, J.S., Huang, Y., Toney, J., Fessenden, J., WoldeGabriel, G., Atudorei, V., Geissman, J.W., Allen, C.D., 2011. Extended megadroughts in the southwestern United States during Pleistocene interglacials. Nature 470, 518–521.
Field, M.H., de Beaulieu, J.L., Guiot, J., Ponel, P., 2000. Middle Pleistocene deposits at La Côte, Val-de-Lans, Isère department, France: plant macrofossil, palynological and fossil insect investigations. Palaeogeogr. Palaeoclimatol. Palaeoecol. 159, 53–83.
Fletcher, W.J., Müller, U.C., Koutsodendris, A., Christanis, K., Pross, J., 2013. A centennial-scale record of vegetation and climate variability from 312 to 240 ka (Marine Isotope Stages 9c–a, 8 and 7e) from Tenaghi Philippon, NE Greece. Quat. Sci. Rev. 78, 108–125.
Follieri, M., Magri, D., Sadori, L., 1988. 250000-year pollen record from Valle di Castiglione (Roma). Pollen Spores 30, 329–356.
Francke, A., Wagner, B., Just, J., Leicher, N., Gromig, R., Baumgarten, H., Vogel, H., Lacey, J.H., Sadori, L., Wonik, T., Leng, M.J., Zanchetta, G., Sulpizio, R., Giaccio, B., 2016. Sedimentological processes and environmental variability at Lake Ohrid (Macedonia, Albania) between 637 ka and the present. Biogeosciences 13, 1179–1196.
Griffiths, H.I., Kryštufek, B., Reed, J.M., 2004. Late Pleistocene rodent dispersal in the Balkans. In: Griffiths, H.I., Kryštufek, B., Reed, J.M. (Eds.), Balkan Biodiversity: Pattern and Process in the European Hotspot. Springer Press, Dordrecht, pp. 135–145.
Grimm, E.C., 1987. CONISS: a FORTRAN 77 program for stratigraphically constrained cluster analysis by the method of incremental sum of squares. Comput. Geosci. 13, 13–35.
Guiot, J., 1990. Methodology of the last climatic cycle reconstruction in France from pollen data. Palaeogeogr. Palaeoclimatol. Palaeoecol. 80, 49–69.
Imeri, A., Mullaj, A., Gjeta, E., Kalajnxhiu, A., Kupe, L., Shehu, J., Dodona, E., 2010. Preliminary results from the study of flora and vegetation of Ohrid lake. Natura Montenegrina 9, 253–264.
Iversen, J., 1944. *Viscum, Hedera* and *Ilex* as climate indicators. Geol. Foren. Stockh. Forh. 66, 463–483.
Joannin, S., Cornée, J.J., Moissette, P., Suc, J.P., Koskeridou, E., Lécuyer, C., Buisine, C., Kouli, K., Ferry, S., 2007. Changes in vegetation and marine environments in the eastern mediterranean (rhodes, Greece) during the early and middle Pleistocene. J. Geol. Soc. 164, 1119–1131.
Jouzel, J., Masson-Delmotte, V., Cattani, O., Dreyfus, G., Falourd, S., Hoffmann, G., Minster, B., Nouet, J., Barnola, J.M., Chappellaz, J., Fischer, H., Gallet, J.C., Johnsen, S., Leuenberger, M., Loulergue, L., Luethi, D., Oerter, H., Parrenin, F., Raisbeck, G., Raynaud, D., Schilt, A., Schwander, J., Selmo, E., Souchez, R., Spahni, R., Stauffer, B., Steffensen, J.P., Stenni, B., Stocker, T.F., Tison, J.L., Werner, M., Wolff, E.W., 2007. Orbital and millennial Antarctic climate variability over the past 800,000 years. Science 317, 793–796.
Just, J., Nowaczyk, N.R., Sagnotti, L., Francke, A., Vogel, H., Lacey, J.H., Wagner, B., 2016. Environmental control on the occurrence of high-coercivity magnetic minerals and formation of iron sulfides in a 640 ka sediment sequence from Lake Ohrid (Balkans). Biogeosciences 13, 2093–2109.
Kandiano, E.S., Bauch, H.A., Fahl, K., Helmke, J.P., Röhl, U., Pérez-Folgado, M., Cacho, I., 2012. The meridional temperature gradient in the eastern North Atlantic during MIS 11 and its link to the ocean–atmosphere system. Palaeogeogr. Palaeoclimatol. Palaeoecol. 333–334, 24–39.
Kandiano, E.S., van der Meer, M.T., Schouten, S., Fahl, K., Sinninghe Damste, J.S., Bauch, H.A., 2017. Response of the North Atlantic surface and intermediate ocean structure to climate warming of MIS 11. Sci. Rep. 7, 46192.
Karner, D.B., Marra, F., Renne, P.R., 2001. The history of the Monti Sabatini and Alban Hills volcanoes: groundwork for assessing volcanic-tectonic hazards for Rome. J. Volcanol. Geoth. Res. 107, 185–219.
Kleinen, T., Hildebrandt, S., Prange, M., Rachmayani, R., Müller, S., Bezrukova, E., Brovkin, V., Tarasov, P.E., 2014. The climate and vegetation of Marine Isotope Stage 11–model results and proxy-based reconstructions at global and regional scale. Quat. Int. 348, 247–265.
Kotthoff, U., Koutsodendris, A., Pross, J., Schmiedl, G., Bornemann, A., Kaul, C., Marino, G., Peyron, O., Schiebel, R., 2011. Impact of Lateglacial cold events on the northern Aegean region reconstructed from marine and terrestrial proxy data. J. Quat. Sci. 26, 86–96.
Koutsodendris, A., Müller, U.C., Pross, J., Brauer, A., Kotthoff, U., Lotter, A.F., 2010. Vegetation dynamics and climate variability during the Holsteinian interglacial based on a pollen record from Dethlingen (northern Germany). Quat. Sci. Rev. 29, 3298–3307.
Koutsodendris, A., Brauer, A., Pälike, H., Müller, U.C., Dulski, P., Lotter, A.F., Pross, J., 2011. Sub-decadal- to decadal-scale climate cyclicity during the Holsteinian interglacial (MIS 11) evidenced in annually laminated sediments. Clim. Past 7, 987–999.
Koutsodendris, A., Pross, J., Müller, U.C., Brauer, A., Fletcher, W.J., Kühl, N., Kirilova, E., Verhagen, F.T.M., Lücke, A., Lotter, A.F., 2012. A short-term climate oscillation during the Holsteinian interglacial (MIS 11c): an analogy to the 8.2ka climatic event? Global Planet. Change 92–93, 224–235.
Koutsodendris, A., Pross, J., Zahn, R., 2014. Exceptional Agulhas leakage prolonged interglacial warmth during MIS 11c in Europe. Paleoceanography 29, 1062–1071.
Koutsodendris, A., Brauer, A., Reed, J.M., Plessen, B., Friedrich, O., Hennrich, B., Zacharias, I., Pross, J., 2017. Climate variability in SE Europe since 1450 AD based on a varved sediment record from Etoliko Lagoon (Western Greece). Quat. Sci. Rev. 159, 63–76.
Lacey, J.H., Francke, A., Leng, M.J., Vane, C.H., Wagner, B., 2015. A high-resolution late glacial to Holocene record of environmental change in the mediterranean from Lake Ohrid (Macedonia/Albania). Int. J. Earth Sci. 104, 1623–1638.
Lacey, J.H., Leng, M.J., Francke, A., Sloane, H.J., Milodowski, A., Vogel, H., Baumgarten, H., Zanchetta, G., Wagner, B., 2016. Northern mediterranean climate since the middle Pleistocene: a 637 ka stable isotope record from Lake Ohrid (Albania/Macedonia). Biogeosciences 13, 1801–1820.
Le Bas, M.J.L., Maitre, R.W.L., Streckeisen, A., Zanettin, B., 1986. A chemical classification of volcanic rocks Based on the total alkali-silica diagram. J. Petrol. 27, 745–750.
Leicher, N., Zanchetta, G., Sulpizio, R., Giaccio, B., Wagner, B., Nomade, S., Francke, A., Del Carlo, P., 2016. First tephrostratigraphic results of the DEEP site record from Lake Ohrid (Macedonia and Albania). Biogeosciences 13, 2151–2178.
Lézine, A.M., von Grafenstein, U., Andersen, N., Belmecheri, S., Bordon, A., Caron, B., Cazet, J.P., Erlenkeuser, H., Fouache, E., Grenier, C., Huntsman-Mapila, P., Hureau-Mazaudier, D., Manelli, D., Mazaud, A., Robert, C., Sulpizio, R., Tiercelin, J.J., Zanchetta, G., Zeqollari, Z., 2010. Lake Ohrid, Albania, provides an exceptional multi-proxy record of environmental changes during the last glacial–interglacial cycle. Palaeogeogr. Palaeoclimatol. Palaeoecol. 287, 116–127.
Lionello, P., Rizzoli-Malanotte, P., Boscolo, R., Alpert, P., Artale, V., Li, L., Luterbacher, J., May, W., Trigo, R., Tsimplis, M., Ulbrich, U., Xoplaki, E., 2006. The mediterranean climate: an overview of the main characteristics and issues. In: Lionello, P., Malanotte-Rizzoli, P., Boscolo, R. (Eds.), Mediterranean Climate Variability. Developments in Earth and Environmental Sciences, 4. Elsevier, Amsterdam, pp. 1–26.
Litt, T., Pickarski, N., Heumann, G., Stockhecke, M., Tzedakis, P.C., 2014. A 600,000 year long continental pollen record from Lake Van, eastern Anatolia (Turkey). Quat. Sci. Rev. 104, 30–41.
Loulergue, L., Schilt, A., Spahni, R., Masson-Delmotte, V., Blunier, T., Lemieux, B., Barnola, J.M., Raynaud, D., Stocker, T.F., Chappellaz, J., 2008. Orbital and millennial-scale features of atmospheric CH_4 over the past 800,000 years. Nature 453, 383–386.
Loutre, M.F., Berger, A., 2003. Marine Isotope Stage 11 as an analogue for the present interglacial. Global Planet. Change 36, 209–217.
Lüthi, D., Le Floch, M., Bereiter, B., Blunier, T., Barnola, J.M., Siegenthaler, U., Raynaud, D., Jouzel, J., Fischer, H., Kawamura, K., Stocker, T.F., 2008. High-resolution carbon dioxide concentration record 650,000-800,000 years before present. Nature 453, 379.
Magri, D., Parra, I., 2002. Late Quaternary western Mediterranean pollen records and African winds. Earth Planet. Sci. Lett. 200, 401–408.
Magri, D., Di Rita, F., Aranbarri, J., Fletcher, W., González-Sampériz, P., 2017. Quaternary disappearance of tree taxa from Southern Europe: timing and trends. Quat. Sci. Rev. 163, 23–55.
Mangili, C., Brauer, A., Plessen, B., Moscariello, A., 2007. Centennial-scale oscillations in oxygen and carbon isotopes of endogenic calcite from a 15,500 varve year record of the Pianico interglacial. Quat. Sci. Rev. 26, 1725–1735.
Marra, F., Sottili, G., Gaeta, M., Giaccio, B., Jicha, B., Masotta, M., Palladino, D.M., Deocampo, D.M., 2014. Major explosive activity in the Monti Sabatini Volcanic District (central Italy) over the 800-390 ka interval: geochronological-geochemical overview and tephrostratigraphic implications. Quat. Sci. Rev. 94, 74–101.
Marra, F., Rohling, E.J., Florindo, F., Jicha, B., Nomade, S., Pereira, A., Renne, P.R., 2016. Independent $^{40}Ar/^{39}Ar$ and ^{14}C age constraints on the last five glacial terminations from the aggradational successions of the Tiber River, Rome (Italy). Earth Planet Sci. Lett. 449, 105–117.
Marra, F., Nomade, S., Pereira, A., Petronio, C., Salari, L., Sottili, G., Bahain, J.J., Boschian, G., Di Stefano, G., Falgueres, C., Florindo, F., Gaeta, M., Giaccio, B., Masotta, M., 2018. A review of the geologic sections and the faunal assemblages of Aurelian Mammal Age of Latium (Italy) in the light of a new chronostratigraphic framework. Quat. Sci. Rev. 181, 173–199.
Martrat, B., Grimalt, J.O., Shackleton, N.J., de Abreu, L., Hutterli, M.A., Stocker, T.F., 2007. Four climate cycles of recurring deep and surface water destabilizations on the Iberian margin. Science 317, 502–507.
Medail, F., Diadema, K., 2009. Glacial refugia influence plant diversity patterns in the Mediterranean Basin. J. Biogeogr. 36, 1333–1345.
Matevski, V., Èarni, A., Avramoski, O., Juvan, N., Kostadinovski, M., Košir, P., Paušiè, A., Šilc, U., 2011. Forest vegetation of Galièica Mountain Range in Macedonia. Založba ZRC Press, Ljubljana.

Matzinger, A., Schmid, M., Veljanoska-Sarafiloska, E., Patceva, S., Guseska, D., Wagner, B., Müller, B., Sturm, M., Wüest, A., 2007. Eutrophication of ancient Lake Ohrid: global warming amplifies detrimental effects of increased nutrient inputs. Limnol. Oceanogr. 52, 338–353.
McManus, J., Oppo, D., Cullen, J., Healey, S., 2003. Marine isotope stage 11 (MIS 11): analog for Holocene and future climate? In: Droxler, A.W., Poore, R.Z., Burckle, L.H. (Eds.), Earth's Climate and Orbital Eccentricity; the Marine Isotope Stage 11 Question. AGU Geophysical Monograph Series 137, pp. 69–85.
Melles, M., Brigham-Grette, J., Minyuk, P.S., Nowaczyk, N.R., Wennrich, V., DeConto, R.M., Anderson, P.M., Andreev, A.A., Coletti, A., Cook, T.L., 2012. 2.8 million years of Arctic climate change from Lake El'gygytgyn, NE Russia. Science 337, 315–320.
Milner, A.M., Roucoux, K.H., Collier, R.E.L., Müller, U.C., Pross, J., Tzedakis, P.C., 2016. Vegetation responses to abrupt climatic changes during the last interglacial complex (marine isotope stage 5) at Tenaghi Philippon, ne Greece. Quat. Sci. Rev. 154, 169–181.
Müller, U.C., Pross, J., Bibus, E., 2003. Vegetation response to rapid climate change in central europe during the past 140,000 yr based on evidence from the Füramoos pollen record. Quat. Res. 59, 235–245.
Müller, U.C., Klotz, S., Geyh, M.A., Pross, J., Bond, G.C., 2005. Cyclic climate fluctuations during the last interglacial in central Europe. Geology 33, 449–452.
Müller, U.C., Pross, J., 2007. Lesson from the past: present insolation minimum holds potential for glacial inception. Quat. Sci. Rev. 26, 3025–3029.
Naafs, B.D.A., Hefter, J., Stein, R., 2014. Dansgaard-Oeschger forcing of sea surface temperature variability in the midlatitude North Atlantic between 500 and 400 ka (MIS 12). Paleoceanography 29, 1024–1030.
Nasri, N., Bojovic, S., Vendramin, G.G., Fady, B., 2007. Population genetic structure of the relict Serbian spruce, *Picea omorika*, inferred from plastid DNA. Plant Systemat. Evol. 271, 1–7.
Nitychoruk, J., Bińka, K., Hoefs, J., Ruppert, H., Schneider, J., 2005. Climate reconstruction for the holsteinian interglacial in eastern Poland and its comparison with isotopic data from marine isotope stage 11. Quat. Sci. Rev. 24, 631–644.
Okuda, M., Yasuda, Y., Setoguchi, T., 2001. Middle to late Pleistocene vegetation history and climatic changes at Lake Kopais, southeast Greece. Boreas 30, 73–82.
Okuda, M., Van Vugt, N., Nakagawa, T., Ikeya, M., Hayashida, A., Yasuda, Y., Setoguchi, T., 2002. Palynological evidence for the astronomical origin of lignite–detritus sequence in the Middle Pleistocene Marathousa Member, Megalopolis, SW Greece. Earth Planet Sci. Lett. 201, 143–157.
Oliveira, D., Desprat, S., Rodrigues, T., Naughton, F., Hodell, D., Trigo, R., Rufino, M., Lopes, C., Abrantes, F., Sánchez Goñi, M.F., 2016. The complexity of millennial-scale variability in southwestern Europe during MIS 11. Quat. Res. 86, 373–387.
Oppo, D.W., McManus, J.F., Cullen, J.L., 1998. Abrupt climate events 500,000 to 340,000 years ago: evidence from subpolar North Atlantic sediments. Science 279, 1335–1338.
Overpeck, J.T., Webb, T., Prentice, I.C., 1985. Quantitative interpretation of fossil pollen spectra: dissimilarity coefficients and the method of modern analogs. Quat. Res. 23, 87–108.
Past Interglacials Working Group of PAGES, 2016. Interglacials of the last 800,000 years. Rev. Geophys. 54, 162–219.
Panagiotopoulos, K., Aufgebauer, A., Schäbitz, F., Wagner, B., 2013. Vegetation and climate history of The lake prespa region since the lateglacial. Quat. Int. 293, 157–169.
Payne, R., Gehrels, M., 2010. The formation of tephra layers in peatlands: an experimental approach. Catena 81, 12–23.
Perini, G., Francalanci, L., Davidson, J.P., Conticelli, S., 2004. Evolution and genesis of magmas from Vico Volcano, Central Italy: multiple differentiation pathways and variable parental magmas. J. Petrol. 45, 139–182.
Peyron, O., Goring, S., Dormoy, I., Kotthoff, U., Pross, J., de Beaulieu, J.L., Drescher-Schneider, R., Vanniere, B., Magny, M., 2011. Holocene seasonality changes in the central Mediterranean region reconstructed from the pollen sequences of Lake Accesa (Italy) and Tenaghi Philippon (Greece). Holocene 21, 131–146.
Peyron, O., Combourieu-Nebout, N., Brayshaw, D., Goring, S., Andrieu-Ponel, V., Desprat, S., Fletcher, W., Gambin, B., Ioakim, C., Joannin, S., Kotthoff, U., Kouli, K., Montade, V., Pross, J., Sadori, L., Magny, M., 2017. Precipitation changes in the Mediterranean basin during the Holocene from terrestrial and marine pollen records: a model–data comparison. Clim. Past 13, 249–265.
Pinti, D.L., Quidelleur, X., Chiesa, S., Ravazzi, C., Gillot, P.-Y., 2001. K–Ar dating of an early Middle Pleistocene distal tephra in the interglacial varved succession of Pianico-Sèllere (Southern Alps, Italy). Earth Planet Sci. Lett. 188, 1–7.
Pol, K., Debret, M., Masson-Delmotte, V., Capron, E., Cattani, O., Dreyfus, G., Falourd, S., Johnsen, S., Jouzel, J., Landais, A., Minster, B., Stenni, B., 2011. Links between MIS 11 millennial to sub-millennial climate variability and long term trends as revealed by new high resolution EPICA Dome C deuterium data – a comparison with the Holocene. Clim. Past 7, 437–450.
Popovska, C., Bonacci, O., 2007. Basic data on the hydrology of lakes Ohrid and prespa. Hydrol. Process. 21, 658–664.
Prentice, I.C., Cramer, W., Harrison, S.P., Leemans, R., Monserud, R.A., Solomon, A.M., 1992. A global biome model based on plant physiology and dominance, soil properties and climate. J. Biogeogr. 19, 117–134.
Prokopenko, A.A., Williams, D.F., Kuzmin, M.I., Karabanov, E.B., Khursevich, G.K., Peck, J.A., 2002. Muted climate variations in continental Siberia during the mid-Pleistocene epoch. Nature 418, 65–68.
Prokopenko, A.A., Bezrukova, E.V., Khursevich, G.K., Solotchina, E.P., Kuzmin, M.I., Tarasov, P.E., 2010. Climate in continental interior Asia during the longest interglacial of the past 500 000 years: the new MIS 11 records from Lake Baikal, SE Siberia. Clim. Past 6, 31–48.
Pross, J., Kotthoff, U., Müller, U.C., Peyron, O., Dormoy, I., Schmiedl, G., Kalaitzidis, S., Smith, A.M., 2009. Massive perturbation in terrestrial ecosystems of the Eastern Mediterranean region associated with the 8.2 kyr B.P. climatic event. Geology 37, 887–890.
Pross, J., Koutsodendris, A., Christanis, K., Fischer, T., Fletcher, W.J., Hardiman, M., Kalaitzidis, S., Knipping, M., Kotthoff, U., Milner, A.M., Müller, U.C., Schmiedl, G., Siavalas, G., Tzedakis, P.C., Wulf, S., 2015. The 1.35-Ma-long terrestrial climate archive of Tenaghi Philippon, northeastern Greece: evolution, exploration, and perspectives for future research. Newsl. Stratigr. 48, 253–276.
Raymo, M.E., Mitrovica, J.X., 2012. Collapse of polar ice sheets during the stage 11 interglacial. Nature 483, 453–456.
Reille, M., Beaulieu, J.L.D., Svobodova, H., Andrieu-Ponel, V., Goeury, C., 2000. Pollen analytical biostratigraphy of the last five climatic cycles from a long continental sequence from the Velay region (Massif Central, France). J. Quat. Sci. 15, 665–685.
Regattieri, E., Giaccio, B., Galli, P., Nomade, S., Peronace, E., Messina, P., Sposato, A., Boschi, C., Gemelli, M., 2016. A multi-proxy record of MIS 11–12 deglaciation and glacial MIS 12 instability from the Sulmona basin (central Italy). Quat. Sci. Rev. 132, 129–145.
Reyes, A.V., Carlson, A.E., Beard, B.L., Hatfield, R.G., Stoner, J.S., Winsor, K., Welke, B., Ullman, D.J., 2014. South Greenland ice-sheet collapse during marine isotope stage 11. Nature 510, 525–528.
Roberts, N., Moreno, A., Valero-Garcés, B.L., Corella, J.P., Jones, M., Allcock, S., Woodbridge, J., Morellon, M., Luterbacher, J., Xoplaki, E., Türkes, M., 2012. Palaeolimnological evidence for an east–west climate see-saw in the Mediterranean since AD 900. Global Planet. Change 84–85, 23–34.
Rodrigues, T., Voelker, A.H.L., Grimalt, J.O., Abrantes, F., Naughton, F., 2011. Iberian Margin sea surface temperature during MIS 15 to 9 (580–300 ka): glacial suborbital variability versus interglacial stability. Paleoceanography 26. PA1204.
Rohling, E.J., Braun, K., Grant, K., Kucera, M., Roberts, A.P., Siddall, M., Trommer, G., 2010. Comparison between Holocene and marine isotope stage 11 sea-level histories. Earth Planet Sci. Lett. 291, 97–105.
Rohling, E.J., Foster, G.L., Grant, K.M., Marino, G., Roberts, A.P., Tamisiea, M.E., Williams, F., 2014. Sea-level and deep-sea-temperature variability over the past 5.3 million years. Nature 508, 477–482.
Rossi, S., 2003. Analisi pollinica della sequenza lacustre di Pianico-Sèllere (Italia). PhD thesis. Université d'Aix Marseille III, France.
Roulleau, E., Pinti, D.L., Rouchon, V., Quidelleur, X., Gillot, P.-Y., 2009. Tephrochronostratigraphy of the lacustrine interglacial record of Pianico, Italian Southern Alps: identifying the volcanic sources using radiogenic isotopes and trace elements. Quat. Int. 204, 31–43.
Rousseau, D.D., Schevin, P., Duzer, D., Cambon, G., Ferrier, J., Jolly, D., Poulsen, U., 2006. New evidence of long distance pollen transport to southern Greenland in late spring. Rev. Palaeobot. Palynol. 141, 277–286.
Ruddiman, W.F., 2005. Cold climate during the closest Stage 11 analog to recent Millennia. Quat. Sci. Rev. 24, 1111–1121.
Saaroni, H., Bitan, A., Alpert, P., Ziv, B., 1996. Continental polar outbreaks into the Levant and eastern Mediterranean. Int. J. Climatol. 16, 1175–1191.
Sadori, L., Koutsodendris, A., Panagiotopoulos, K., Masi, A., Bertini, A., Combourieu-Nebout, N., Francke, A., Kouli, K., Joannin, S., Mercuri, A.M., Peyron, O., Torri, P., Wagner, B., Zanchetta, G., Sinopoli, G., Donders, T.H., 2016. Pollen-based paleoenvironmental and paleoclimatic change at Lake Ohrid (south-eastern Europe) during the past 500 ka. Biogeosciences 13, 1423–1437.
San-Miguel-Ayanz, J., de Rigo, D., Caudullo, G., Houston Durrant, T., Mauri, A. (Eds.), 2016. European Atlas of Forest Tree Species. Publication Office of the European Union, Luxembourg.
Sinopoli, G., Masi, A., Regattieri, E., Wagner, B., Francke, A., Peyron, O., Sadori, L., 2018. Palynology of the last interglacial complex at Lake Ohrid: palaeoenvironmental and palaeoclimatic inferences. Quat. Sci. Rev. 180, 177–192.
Stein, R., Hefter, J., Grützner, J., Voelker, A., Naafs, B.D.A., 2009. Variability of surface water characteristics and heinrich-like events in the Pleistocene midlatitude North Atlantic ocean: biomarker and XRD records from IODP site U1313 (MIS 16–9). Paleoceanography 24. PA2203.
Svenning, J.C., 2003. Deterministic Plio-Pleistocene extinctions in the European cool-temperate tree flora. Ecol. Lett. 6, 646–653.
Sykes, M.T., Prentice, I.C., Cramer, W., 1996. A bioclimatic model for the potential distributions of North European tree species under present and future Climates. J. Biogeogr. 23, 203–233.
Tarasov, P.E., Nakagawa, T., Demske, D., Österle, H., Igarashi, Y., Kitagawa, J., Mokhova, L., Bazarova, V., Okuda, M., Gotanda, K., Miyoshi, N., Fujiki, T., Takemura, K., Yonenobu, H., Fleck, A., 2011. Progress in the reconstruction of Quaternary climate dynamics in the Northwest Pacific: a new modern analogue reference dataset and its application to the 430-kyr pollen record from Lake Biwa. Earth Sci. Rev. 108, 64–79.
Tye, G.J., Sherriff, J., Candy, I., Coxon, P., Palmer, A., McClymont, E.L., Schreve, D.C., 2016. The $\delta^{18}O$ stratigraphy of the Hoxnian lacustrine sequence at Marks Tey, Essex, UK: implications for the climatic structure of MIS 11 in Britain. J. Quat. Sci. 31, 75–92.
Tzedakis, P.C., 2007. Seven ambiguities in the Mediterranean palaeoenvironmental narrative. Quat. Sci. Rev. 26, 2042–2066.
Tzedakis, P., Andrieu, V., De Beaulieu, J.-L., Birks, H., Crowhurst, S., Follieri, M., Hooghiemstra, H., Magri, D., Reille, M., Sadori, L., 2001. Establishing a terrestrial chronological framework as a basis for biostratigraphical comparisons. Quat.

Sci. Rev. 20, 1583–1592.
Tzedakis, P.C., McManus, J.F., Hooghiemstra, H., Oppo, D.W., Wijmstra, T.A., 2003. Comparison of changes in vegetation in northeast Greece with records of climate variability on orbital and suborbital frequencies over the last 450 000 years. Earth Planet Sci. Lett. 212, 197–212.
Tzedakis, P., Roucoux, K., De Abreu, L., Shackleton, N., 2004. The duration of forest stages in southern Europe and interglacial climate variability. Science 306, 2231–2235.
Tzedakis, P.C., Hooghiemstra, H., Pälike, H., 2006. The last 1.35 million years at Tenaghi Philippon: revised chronostratigraphy and long-term vegetation trends. Quat. Sci. Rev. 25, 3416–3430.
Tzedakis, P.C., Pälike, H., Roucoux, K.H., de Abreu, L., 2009. Atmospheric methane, southern European vegetation and low-mid latitude links on orbital and millennial timescales. Earth Planet Sci. Lett. 277, 307–317.
van der Wiel, A.M., Wijmstra, T.A., 1987. Palynology of the lower part (78-120 m) of the core Tenaghi Philippon ii, middle Pleistocene of Macedonia, Greece. Rev. Palaebot. Palynol. 52, 73–88.
Voelker, A.H.L., Rodrigues, T., Billups, K., Oppo, D., McManus, J., Stein, R., Hefter, J., Grimalt, J.O., 2010. Variations in mid-latitude North Atlantic surface water properties during the mid-Brunhes (MIS 9–14) and their implications for the thermohaline circulation. Clim. Past 6, 531–552.
Vogel, H., Wagner, B., Zanchetta, G., Sulpizio, R., Rosén, P., 2010. A paleoclimate record with tephrochronological age control for the last glacial-interglacial cycle from Lake Ohrid, Albania and Macedonia. J. Paleolimnol. 44, 295–310.
Wagner, B., Vogel, H., Zanchetta, G., Sulpizio, R., 2010. Environmental change within the Balkan region during the past ca. 50 ka recorded in the sediments from lakes Prespa and Ohrid. Biogeosciences 7, 3187–3198.
Wagner, B., Wilke, T., Francke, A., Albrecht, C., Baumgarten, H., Bertini, A., Combourieu-Nebout, N., Cvetkoska, A., D'Addabbo, M., Donders, T.H., Föller, K., Giaccio, B., Grazhdani, A., Hauffe, T., Holtvoeth, J., Joannin, S., Jovanovska, E., Just, J., Kouli, K., Koutsodendris, A., Krastel, S., Lacey, J.H., Leicher, N., Leng, M.J., Levkov, Z., Lindhorst, K., Masi, A., Mercuri, A.M., Nomade, S., Nowaczyk, N., Panagiotopoulos, K., Peyron, O., Reed, J.M., Regattieri, E., Sadori, L., Sagnotti, L., Stelbrink, B., Sulpizio, R., Tofilovska, S., Torri, P., Vogel, H., Wagner, T., Wagner-Cremer, F., Wolff, G.A., Wonik, T., Zanchetta, G., Zhang, X.S., 2017. The environmental and evolutionary history of Lake Ohrid (FYROM/Albania): interim results from the SCOPSCO deep drilling project. Biogeosciences 14, 2033–2054.
Wanner, H., Brönnimann, S., Casty, C., Gyalistras, D., Luterbacher, J., Schmutz, C., Stephenson, D.B., Xoplaki, E., 2001. North Atlantic oscillation–concepts and studies. Surv. Geophys. 22, 321–381.
Wardle, D.A., Walker, L.R., Bardgett, R.D., 2004. Ecosystem properties and forest decline in contrasting long-term chronosequences. Science 305, 509–513.
Wijmstra, T.A., Smit, A., 1976. Palynology of the middle part (30–78 metres) of the 120 m deep section in northern Greece (Macedonia). Plant Biol. 25, 297–312.
Wulf, S., Hardiman, M., Staff, R.A., Koutsodendris, A., Appelt, O., Blockley, S.P.E., Lowe, J.J., Manning, C.J., Ottolini, L., Schmitt, A.K., Smith, V.C., Tomlinson, E.L., Vakhrameeva, P., Knipping, M., Kotthoff, U., Milner, A.M., Müller, U.C., Christanis, K., Kalaitzidis, S., Tzedakis, C., Schmiedl, G., Pross, J., 2018. The marine isotope stage 1 – 5 cryptotephra record of Tenaghi Philippon, Greece: towards a detailed tephrostratigraphic framework for the Eastern Mediterranean region. Quat. Sci. Rev. 186, 236–262.
Xoplaki, E., González-Rouco, J.F., Luterbacher, J., Wanner, H., 2004. Wet season Mediterranean precipitation variability: influence of large-scale dynamics and trends. Clim. Dynam. 23, 63–78.
Yin, Q., Berger, A., 2015. Interglacial analogues of the Holocene and its natural near future. Quat. Sci. Rev. 120, 28–46.